# Holistic method for determining the techno-economic feasibility of waste heat for the planning of the low-temperature district heating systems

**Josip Miškić*[1], Hrvoje Dorotić[2], Tomislav Pukšec[1], Daniel Rolph Schneider[1], Neven Duić[1]**

[1] *The University of Zagreb, Faculty of Mechanical Engineering and Naval Architecture, Department of Energy, Power Engineering and Environmental Engineering, Ivana Lučića 5, 10002, Zagreb, Croatia*

[2] *Energy Institute Hrvoje Požar, Savska cesta 163, 10000, Zagreb. Croatia*

**email: josip.miskic@fsb.unizg.hr*

**Abstract**

The heating sector is the most energy-intensive sectors, accounting for almost 50% of final energy consumption at the EU and almost 70% of that energy comes from fossil fuels. Urban waste heat sources, the refrigeration system of supermarkets, cooling systems of supermarkets, shopping malls, data centres, and power substations are known as systems that can be heat sources for the district heating (DH) system. This paper presents a holistic method to assess the economic, energy, and environmental benefits of integrating urban waste heat sources into DH. The method considers different boundary conditions and compares these systems to individual natural gas boilers, as well as to DH based on natural gas boilers. The observed boundary conditions include varying temperature regimes of the DH network, heat demands, different shares of space heating, and plot ratios. The method has been implemented and tested in the case of Zagreb. The results showed that Low-Temperature DH is viable for lower plot ratio and high heat demand, while Neutral-temperature DH are suitable for high plot ratio and high heat demand. Ultra Low-Temperature DH is viable for medium plot ratio and medium heat demand. The conventional solutions remain viable for low plot ratio and low heat demand.

**Keywords:** *district heating, urban waste heat sources, waste heat potential, techno-economic feasibility, district heating planning*

## HIGHLIGHTS

- 3E assessment of integrating urban waste heat sources into the low-temperature DH system.
- 4th and 5th generation DHC are economically, energy, and environmentally viable compared to individual solutions.
- NTDH is viable for a high plot ratio and high heat demand, while LTDH is for a low plot ratio and high heat demand.
- Conventional solutions remain viable for low plot ratios and low heat demand.

| Abbreviations | |
|---|---|
| 3E | Economic, Energy, and Environmental |
| BTES | Borehole Thermal Energy Storage |
| CEF | Carbon Emission Factor |
| COP | Coefficient of Performance |
| $CO_2$ | Carbon dioxide |
| DH | District Heating |
| DHC | District Heating and Cooling |
| DHW | Domestic Hot Water |
| ETS | Emission Trading System |
| GHG | Greenhouses Gas |
| GIS | Geographical Information System |
| HD | Heat Demand |
| HP | Heat Pump |
| LCOH | Levelised Cost of Heat |
| LHDD | Linear Heat Demand Density |
| LTDH | Low-temperature District Heating |
| O&M | Operation and Maintenance |
| NTDH | Neutral-temperature District Heating |
| PEF | Primary Energy Factor |
| PR | Plot ratio |
| PTES | Pit Thermal Energy Storage |
| SH | Space Heating |
| TES | Thermal Energy Storage |
| ULTDH | Ultra low-temperature District Heating |

| Symbols | | |
|---|---|---|
| $A_B$ | Budiling area | $m^2$ |
| $A_D$ | District area | $m^2$ |
| $CAPEX$ | Capital expenditures | € |
| $CRF$ | Capital recovery factor | – |
| $E$ | Electricty cost | € |
| $f_{CO_2}$ | Carbon emission factor | $\frac{tCO_2}{MWh}$ |
| $f_{prim}$ | Primary energy factor | – |
| $G$ | Gas cost | € |
| $I$ | Investment cost | € |
| $i$ | Discount rate | % |
| $n$ | Equipment lifetime | – |
| $OPEX$ | Operating expenditures | € |
| $PR$ | Plot ratio | – |
| $Q_{SH}$ | Total heat demand for space heating | $\frac{MWH}{a}$ |
| $Q_{DHW}$ | Total annual heat demand for domestic how water preparation | $\frac{MWH}{a}$ |
| $SH_s$ | Space heating share | % |

## 1. Introduction

Urbanization is rapidly increasing, which brings the challenge of managing waste heat from urban sources like data centres, supermarkets, shopping malls, and wastewater treatment plants. If not managed effectively, this waste heat can lead to urban heat islands and negatively impact the environment. One promising solution is integrating this waste heat into district heating (DH) systems, a method that has already shown beneficial results. Integrating urban waste heat sources into DH systems can significantly reduce greenhouse gas (GHG) emissions and energy consumption. An important factor for successful integration is the spatial distribution of these heat sources and their temporal availability. This article focuses on the first challenge: spatial distribution. Spatial distribution analysis typically involves urban waste heat mapping, a technique used to identify and quantify waste heat sources from various urban activities. It provides a spatial overview of the urban heat island effect and highlights areas where waste heat recovery is most viable. In the following section, we present a review of studies addressing similar challenges.

To achieve the comprehensive goal of decarbonization, Lund et al. in [1] propose the implementation of the DH network for the fourth ($4^{th}$) and fifth ($5^{th}$) generations. For this purpose, they identified differences and similarities between the $4^{th}$ DH and $5^{th}$ district heating and cooling (DHC) generation regarding aims and abilities. Volkova et al. [2] applied a multi-criteria analysis method to quantify the main identified barriers and drivers behind the implementation of $5^{th}$ generation DHC systems in Baltic areas. The new urban areas in the Baltic states are being developed with low-energy buildings so $5^{th}$ generation DHC systems can be integrated to supply heat. They showed that the use of heat pumps combined with excess heat opened an opportunity for $5^{th}$ generation DHC. Meesenburg et al. [3] compared the economic feasibility of three Ultra Low-temperature District Heating (ULTDH) systems to Low-temperature District Heating (LTDH) systems which are both characteristics of the $4^{th}$ DH and $5^{th}$ DHC systems. They compared different solutions based on Levelized Cost of Heat (LCOH), socioeconomic net present value, and overall seasonal coefficient of performance. They showed that LTDH is usually economically viable, while ULTDH could be viable if the linear heat demand density (LHDD) is high. A similar comparison is carried out by Gudmundsson et al. in [4] where authors aimed to compare the LCOH from $4^{th}$ and $5^{th}$ generation DHC systems and found out that $4^{th}$ generation is the more feasible option in cold and moderate climates. They showed that the $5^{th}$ DHC system supply temperature is insufficient to fulfil heat demand (HD). In the case of $5^{th}$ DHC systems, there is a need for additional investment costs for end-users due to the heat pump installation for boosting supply temperature at the required level for the buildings. In [5] Buffa et al. analyse 40 European thermal networks using heat pumps to provide both heating and cooling. The authors found that high performance and low non-renewable primary energy factors are achieved if renewable and urban waste heat is used. This allows $5^{th}$ generation DHC systems to be extended up to the district scale while achieving low primary energy factors and exploiting a multitude of local urban heat sources. In [6] Buonomano et al. proposed a simulation tool for the design and the optimisation of $5^{th}$ generation DHC systems. They investigated an innovative predictive control logic to optimise water loop temperature which showed that by this principle significant primary energy savings, 6,5%, can be achieved.

In [7] Jodeiri et al. reviewed the technical and non-technical difficulties associated with the exploitation of solar thermal, waste heat, geothermal, and biomass as an energy source in DH systems. Also, the authors highlighted the importance of seasonal storage for the maximization of renewable energy uptake. Yuan et al. [8] focused on renewable energy and waste heat potential in DH systems in China. The paper highlighted the synergy of RES, waste heat, and thermal storage technologies in DH through increased energy efficiency, as well as a more economically viable pathway to the smart energy system. Dorotić et al. [9] developed an economic assessment model for the integration of urban waste heat sources into DH systems based on the pinch point and LCOH method. The authors observed supermarkets and power substations as urban waste heat sources. They showed that supermarkets are a relatively inexpensive waste heat source and that there is no influence of the DH temperature regime on results, while power substations are expensive sources. However, the cost of power substations can be lowered by lowering the DH temperature regime. Huang et al. [10] explored the techno-economic feasibility of heat recovery from a supermarket refrigeration system (SRS) with a heat recovery unit in terms of designing a dynamic heat recovery control and business models. They developed two business models with whom they proved that heat recovery from SRS achieves energy cost savings from 41% to 93%. Giunta et al. [11] investigated the utilization of the waste heat from $CO_2$ refrigeration systems in supermarkets. The authors presented two control strategies that showed that supermarkets can profit up to 10.000,00 € per year by selling the heat while achieving an 18% reduction of $CO_2$ emissions per year. Stock et al. in [12] developed optimisation model that considers refurbishment for buildings and the installation of heat pumps to optimise the integration of low-temperature heat sources into existing DH systems is presented. Their results showed that waste heat integration through decentral heat pumps reduces the operational cost by 6,4% and refurbishment cost by 24,4%.

Energy mapping techniques are used to estimate the local area energy demand, a basis on which the DH system network designers will rely. Brocklebank et al. [13] presented heat mapping for DH network predesign in the local area. The authors showed that if there is enough HD implementation of DH is suitable. Su et al. [14] mapped the geolocations and the technical potentials of the clean non-fossil fuel heat sources for densely populated regions, using a Geographical Information System (GIS) based integrative analysis method for Stockholm City. The results showed that there are enough clean and non-fossil heat sources that will satisfy 100% of the existing DH requirements. Novosel et al. [15] presented an HD mapping and DH viability assessment method using public databases. They presented a three-step method: aggregated HD assessment, bottom-up mapping, and top-down mapping. The method showed that in the Case of Croatia, there is significant potential for the economic utilization of district heating. Chambers et al. [16] presented an analysis of the potential for the supply of DH systems using high and low network temperatures. A spatial clustering method is used to link potential supplies and demands, and monthly supply and demand curves are used to calculate the potential for supply subject to spatiotemporal constraints. Persson and Werner [17] presented a concept for assessing network investment cost levels for DH systems based on LHDD. They showed that the future capital cost for DH in the cities is low since they are dens, especially for large cities and inner-city areas. Nielsen and Moller [18] focused on developing a method for assessing the costs associated with supplying heat with DH. Authors showed that DH economic feasibility depends on area to area, but also on reduction in production cost, transmission, and distribution losses. Buhler et al. [19] presented a geographical mapping of excess heat. Based on this mapping, a systematic approach for identifying cases for the utilization of excess heat is proposed. The results from this paper showed how the spatial mapping of excess heat sources can be used to identify their utilization potentials. The identified case studies show that it can be economically feasible to connect the heat sources to the DH systems.

This paper aims to address several research gaps in the existing literature. From the above-mentioned research studies, it was noticed that many studies focus only on the economic and energy feasibility of integrating urban waste heat sources into DH systems. These studies also explore the role of GIS approaches in this process. However, these studies usually concentrate on a single specific urban waste heat source. As a result, they do not offer a complete, holistic method that could be applied to various areas and a wide range of urban waste heat sources. This novel method would enable easier planning of the construction and expansion of low temperature DH systems. Therefore, the novelty of this paper which aims to develop a holistic method is:

- Systematic comparison of multiple DH configurations, including LTDH, NTDH, and ULTDH, against conventional natural gas-based solutions.
- Scenario analysis using the method reveals how changes in urban density, heat demand, and other boundary conditions impact the viability of each system.
- Insights into the feasibility of urban waste heat utilization, from a wide range of urban waste heat sources in different urban settings.
  Identification of locations with high potential to implement 4$^{th}$ and 5$^{th}$ generation DHC systems.

This paper is structured as follows. Section 2 presents the method: spatial analysis, thermodynamic models of the urban waste heat sources, DH system model, economic analysis, and energy and environmental analysis. In Section 3 the input data for the method are presented. In Section 3 the results are presented which are discussed in Section 4. Finally, in Section 5 the Conclusion and Discussion are given.

## 2. Method

This section introduces a novel holistic method designed to assess the economic costs as well as the energy and environmental benefits of integrating urban waste heat sources into DH systems. The method accounts for various boundary conditions. Additionally, it compares these systems to individual natural gas boilers used in both single-family houses and multi-story residential buildings. It also evaluates DH systems that rely on natural gas boilers. The observed boundary conditions are:

- Different low-temperature regimes of the DH network (low-, ultralow-, and neutral-DH).
- Different waste heat sources with their characteristics (quantity, quality, availability, etc.).
- Different heat demands (environments with low and high demand).
- Different plot ratios (PR) (high and low built environments).
- Different space heating shares ($SH_S$) (high and low energy efficient buildings).

To vary different boundary conditions, it is necessary to conduct scenario analysis based on changes in district area, as district area is a parameter that affects PR, HD, $SH_S$, and urban waste heat sources that will be integrated into the DH network. The scenario analysis approach is presented in Section 3.

The four-step holistic method and setup are shown in Figure 1.

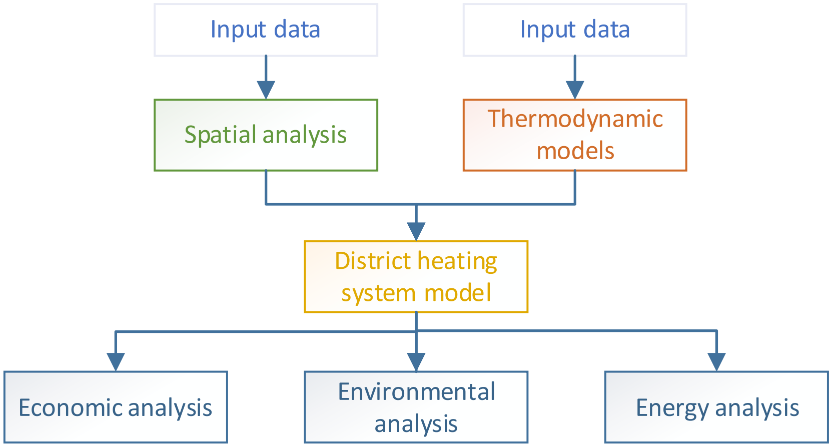


*Figure 1 The method for determining the radius of the techno-economic feasibility of the urban waste heat integration into the low-temperature DH systems*

In the first step, a spatial analysis is performed for the selected case study location. This analysis is used to conduct scenario analysis, dividing the case study area into districts. Three district scenarios are considered, which are explained later in the paper. The spatial analysis considers key characteristics of the location, such as the position of urban waste heat sources (supermarkets, shopping malls, power substations, data centres), district areas, total building floor areas, heated floor areas, and HD. The main result of this analysis is the PR.

In the second step, a thermodynamic analysis of the urban waste heat sources is performed. Temperature distribution and potential are calculated using thermodynamic models for these sources. This analysis determines the available waste heat for integration into the DH network. The calculations are done on an hourly basis.

The results from the first two steps provide input data for the third step, which is the dimensioning of the DH system. This step considers various parameters such as PR, HD, network heat losses, pumping power, and the coefficient of performance (COP) for heat pumps (HP).

In the fourth and final step, a 3E analysis is conducted. The economic analysis uses the LCOH method, while the energy and environmental analysis is carried out using the Primary Energy Factor (PEF) and Carbon Emission Factor (CEF).

The focus of this method is on the central part of the DH system, specifically the production units (supply units). This helps to better understand their impact on economic feasibility, energy performance, and environmental impact. In addition to the supply side, the method also considers the distribution network. According to the E.ON ectogrid™ concept [20], in 5th generation DH systems, the DH operator typically owns both the supply units and the distribution network. However, the customer is responsible for the equipment on the demand side, such as end-user substations. For this reason, end-user substations were excluded from the analysis.

### 2.1. Spatial analysis

Spatial analysis in QGIS allows for the mapping and assessment of urban waste heat sources. It focuses particularly on cooling systems in supermarkets, shopping malls, transformer stations, data centres, and supermarket refrigeration systems. The analysis includes several key components, such as the calculation of PR, HD, and $SH_S$. These factors contribute to a better understanding of urban energy dynamics and potential heat recovery opportunities. In this paper, the emphasis is on cooling systems in supermarkets, shopping malls, transformer stations, data centres, and supermarket refrigeration systems.

The workflow of the spatial analysis is shown in Figure 2.

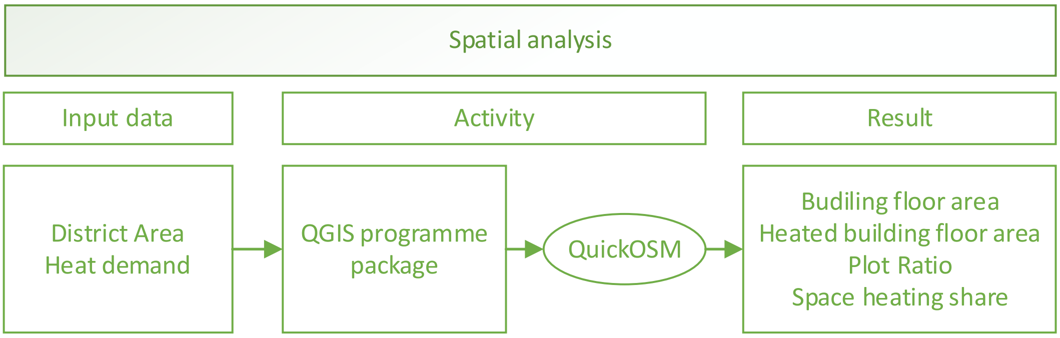


*Figure 2 Workflow of the spatial analysis*

Firstly, the spatial analysis starts by using geospatial data layers such as satellite imagery, land use data, and infrastructure maps. QGIS is used to identify and visualize urban areas that host significant waste heat sources. By overlaying data on the locations of supermarkets, shopping malls, transformer stations, data centres, and other relevant facilities, researchers can pinpoint areas where waste heat generation is prominent. Next, the PR is calculated to assess the intensity of urban development in specific areas.

The PR, also known as the floor area ratio, is calculated by dividing the total floor area of buildings, $A_B$, within a defined district area by the total district area, $A_D$.

$$PR = \frac{A_B}{A_D}, [-] \tag{1}$$

According to Persson and Werner [17] [21], PR usually varies from 0 to 2. Higher values indicate inner city areas with higher building density, such as multi-story residential houses, business buildings, and towers. Lower values represent outer city areas with lower building density, including smaller multi-story buildings and single-family houses.

This calculation provides valuable information about urban density and building utilization, which can be further analysed to understand the distribution of HD within urban areas. After calculating PR, the analysis shifts to estimating HD in the urban environment. Various data sources, such as building footprints, land use classifications, and population density, are used to estimate the total energy demand for space heating (SH) in a given area [15].

Using spatial interpolation techniques and statistical modelling, HD can be estimated at a granular level. This allows the identification of areas with high heating requirements. Lastly, the spatial analysis assesses the share of SH within the total energy demand of urban areas. By comparing the HD for SH with the overall energy demand in a specific area, the space heating share can be calculated using the following equation.

$$SH_s = \frac{Q_{SH}}{Q_{DHW} + Q_{SH}}, [-] \tag{2}$$

Where $Q_{SH}$ presents the total annual HD for SH and $Q_{DHW}$ total annual HD for preparing DHW. $SH_S$ can vary from 0,1 to 0,95, representing different building energy efficiencies. Lower $SH_S$ present buildings with high energy efficiency while higher $SH_S$ values present low energy efficiency values.

Spatial analysis in QGIS provides a framework for mapping urban waste heat sources. It helps in calculating PR, estimating HD, and assessing the SH in urban energy consumption. By using geographic data and spatial analysis techniques, QGIS identifies suitable locations for waste heat recovery. It also assesses HD characteristics. This approach enables efficient integration of urban waste heat sources into DH systems, enhancing energy efficiency and sustainability.

### 2.2. Urban waste heat thermodynamic models

Thermodynamic models of urban waste heat sources include the cooling systems of supermarkets, shopping malls, power substations, and data centres. They also encompass the refrigeration systems of supermarkets. These models were developed based on available research and a review of existing databases. To perform calculations, the models require input data that depend on the type and purpose of the building. The main outputs of the thermodynamic models are the distribution of temperature and the potential waste heat from an urban source. Additionally, these models operate on an hourly scale.

Figure 3 shows the workflow of thermodynamic models.

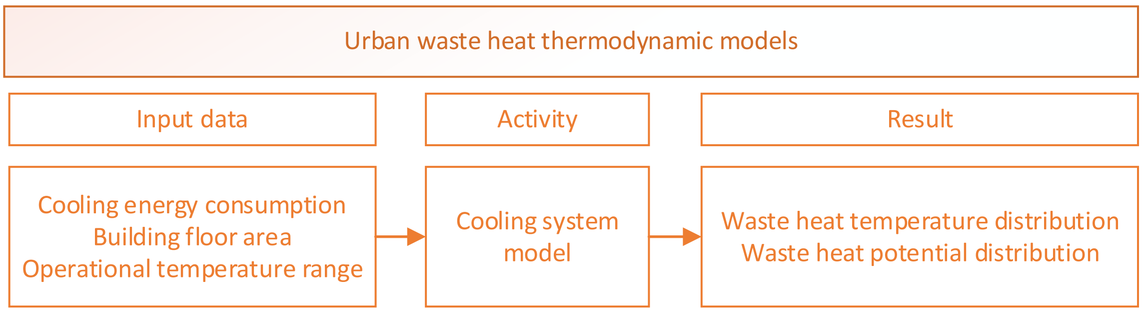


*Figure 3 Workflow of thermodynamic models*

To determine the thermodynamic models of supermarket cooling and refrigeration, shopping malls, data centres, and power substation cooling systems the approach developed by authors in [9] and [22] is used.

### 2.3. DH system model

A DH system model was developed to determine when integrating urban waste heat sources is economically feasible. The calculation of HD, DH network investment, heat loss, and pumping power was not based on a detailed network analysis. Instead, it relied on estimates from existing DH networks. Figure 4 presents a simplified DH system, consisting of three main components: heat energy producers, heat networks, and end users. Producers are responsible for generating enough thermal energy to meet the needs of end users. The DH network distributes heat from the producer to the end user.

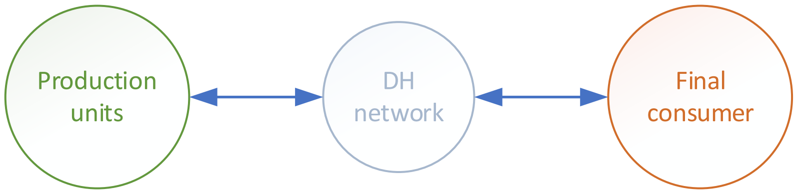


*Figure 4 Simplified DH system*

Figure 5 shows the workflow model of the DH system. Based on the input data, the model calculates the amount of waste heat that can be integrated into the DH network at an hourly level. It also determines the production capacity of the backup unit. This paper examines how the size of the district impacts the results of the economic analysis.

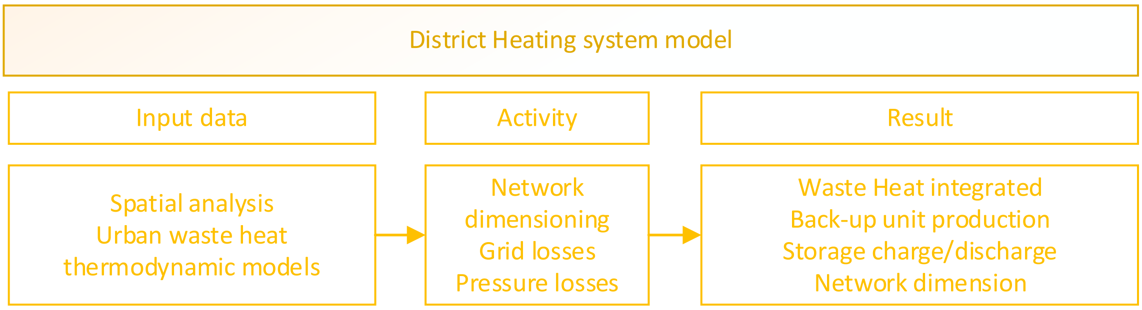


*Figure 5 DH system model workflow*

The network investment cost was calculated based on several factors. These include the PR, specific HD, effective width, and estimated average pipe diameter. The calculation method follows the approach developed by Meesenburg et al. [3] and by Persson et Werner [21].

### 2.4. 3E analysis

The 3E analysis, which includes the energy, economic, and environmental aspects, offers a comprehensive way to assess heating systems. It focuses on key factors such as the Levelized Cost of Heat, Primary Energy Coefficient, and Carbon Emission Factor. By integrating these three dimensions, the method provides a complete view of the sustainability and performance of DH systems.

Considering energy efficiency, economic feasibility, and environmental impact together enables decision-makers to make well-informed choices. This approach ensures a balance between technical feasibility, financial viability, and environmental responsibility in the shift toward more sustainable DH solutions. The 3E analysis is conducted on an annual basis.

#### 2.4.1. Economic evaluation

Economic analysis focuses on the cost implications associated with different DH systems over their lifecycle. The LCOH is a parameter that is used to assess the cost of total annual HD. It is calculated as a ratio of $CAPEX$ and $OPEX$ sum to total annual HD. The value of $LCOH$ is important when it comes to comparing energy systems that use different energy sources and technologies as its "levels" their values to a comparable degree.

$$LCOH = \frac{CAPEX+OPEX}{\dot{Q}_{tot}}, [\frac{€}{MWh}] \quad (3)$$

Capital expenditures ($CAPEX$) can be calculated by multiplying the capital recovery factor ($CRF$) with the investment cost $I$ of a certain element of a network (e.g., central HP). The capital recovery factor is used to calculate the present value of a series of equal annual cash payments which for the needs of this paper equals $CAPEX$. The value $n$ represents the lifetime (in years) of a certain part of a system, while the value $i$ represents the discount rate.

$$CAPEX = CRF * I = \frac{i * (1+i)^n}{(1+i)^n - 1} * I, [€] \quad (4)$$

Operating expenditures ($OPEX$) of a system (e.g., DH network) can be calculated as a sum of operational and management costs (O&M) and electricity and/or gas consumption costs. These costs are ongoing throughout the year and can be calculated daily, weekly basis, or simply annual basis. O&M costs include inventory costs, repairs, overhauls, electricity ($E$) and/or gas ($G$) costs of all parts of the network, pay checks for employees, etc.

$$OPEX = \sum_{i=1}^{N} O\&M_i + E_i + G_i, [€] \quad (5)$$

### 2.4.2. Energy and Environmental evaluation

Environmental analysis examines the carbon footprint and other environmental impacts of DH technologies. Carbon Emission Factor ($f_{CO_2}$) indicates how much $CO_2$ gasses were emitted into the atmosphere to generate a unit of electricity or a unit of usable thermal energy. The value of $f_{CO_2}$ can be calculated for each scenario that differs from others in energy consumption. First, total electricity or gas consumption was converted to the equivalent amount of carbon dioxide emissions. The result was then divided into total annual HD to calculate the $CEF$ of each scenario.

$$f_{CO_2} = \frac{(\dot{W}_{tot} \ or \ \dot{T}_{tot}) * f_{CO_2}}{\dot{Q}_{tot}}, [\frac{tCO_2}{MWh}] \quad (6)$$

Energy analysis within this framework involves assessing the efficiency and consumption patterns of heating technologies. A primary energy factor ($f_{prim}$) indicates how much primary energy is used to generate a unit of electricity or a unit of usable thermal energy. The value of $f_{prim}$ can be calculated for each scenario that differs from others in energy consumption. First, total electricity or gas consumption was converted to primary energy. The result was then divided into total annual HD to calculate the $f_{prim}$ of each scenario.

$$f_{prim} = \frac{(\dot{W}_{tot} \ or \ \dot{T}_{tot}) * f_{prim}}{\dot{Q}_{tot}}, [-] \quad (7)$$

The PEF, representing the ratio of primary energy input to final energy output, provides insight into the overall energy efficiency of a system by considering energy losses throughout the entire supply chain, from extraction to end-use.

## 2.5. Case study

The method was applied in the City of Zagreb, Croatia. Zagreb was chosen for two main reasons. First, it represents nearly 20% of Croatia's total population. Second, it accounts for 23% of the total heat demand at the national level. The method is applied as follows.

As explained in Section 2, a scenario analysis was conducted to examine the boundary conditions. For this analysis, the city was divided into districts. This division was achieved through a scaling procedure. The number of districts increased linearly, as shown in Figure 6. Besides this, Figure 6 shows the district area Scenarios versus the number and area of districts.

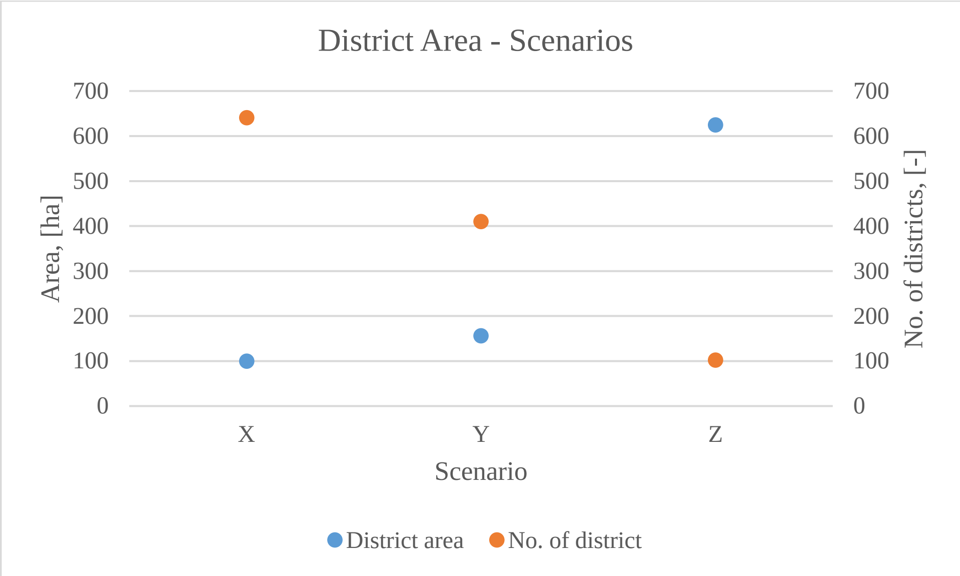


*Figure 6 City of Zagreb - District Area Scenarios*

Therefore, three district area scenarios are defined X, Y, and Z:

- Scenario X – District area of 100 ha (1000x1000 m).
- Scenario Y – District area of 156 ha (1250x1250 m).
- Scenario Z – District area of 625 ha (2500x2500 m).

Figure 7 shows the division into the districts for Scenario X – a), Y – b), and Z – c) and the district area in the scenario.

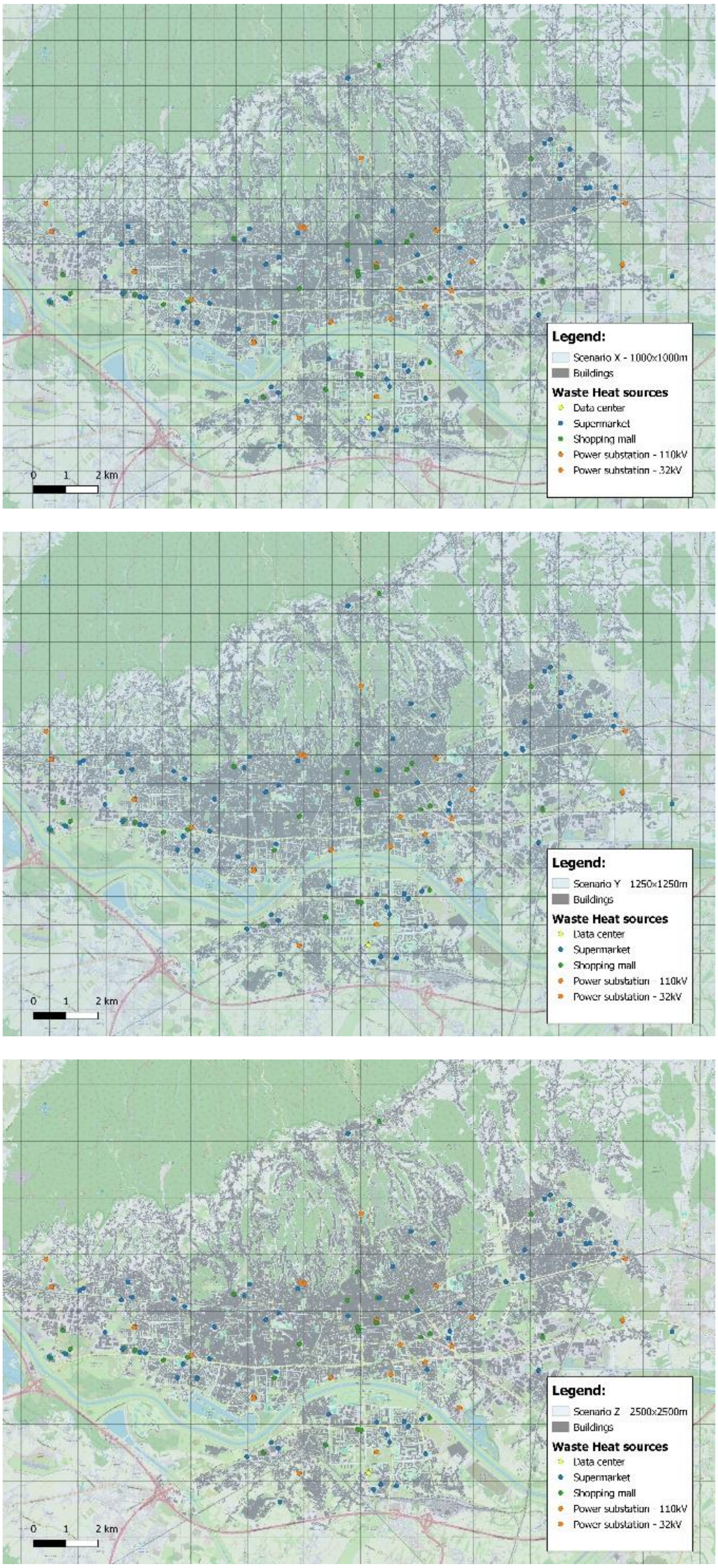


***a)***

***b)***

***c)***

*Figure 7 City of Zagreb – Scenario X, Y, Z*

For each district scenario, different DH system configurations were analysed considering different DH network temperature regimes. Figure 8 presents variations of the DH system configuration, one without thermal energy storage (TES), Figure 8 – a), and one with TES, Figure 8 – b). Two types of thermal energy storage were considered, Pit Thermal Energy Storage (PTES) and Borehole Thermal Energy Storage (BTES). In each scenario, the central source is a waste heat source, connected with a HP to the network. As a backup unit HP is set.

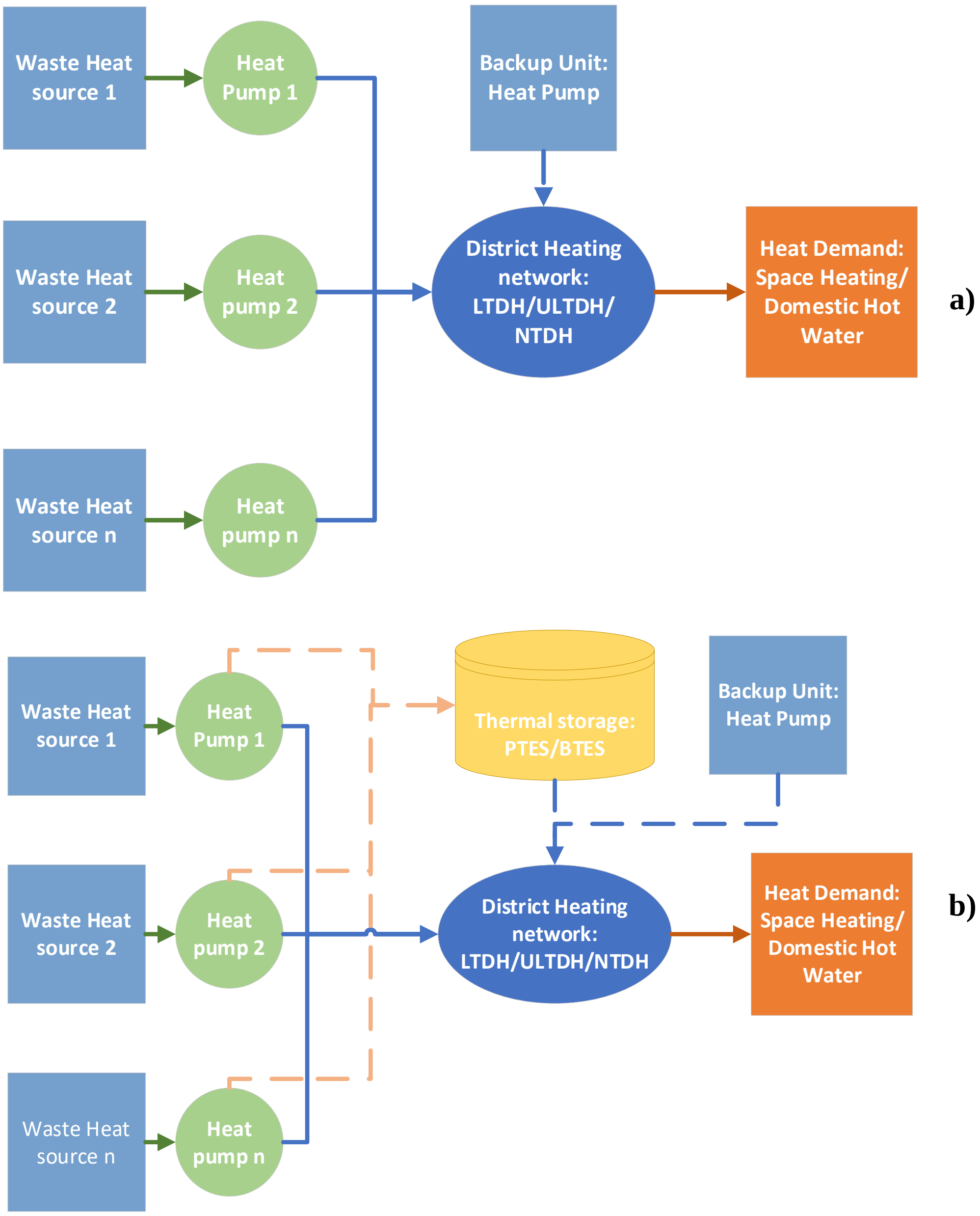


*Figure 8 DH system configurations: a) without TES, b) with TES*

Table 1 shows all scenarios and their characteristics regarding district scenario, network type, central heat source, backup unit source, and thermal storage type. In the final column accompanying label is presented.

*Table 1 Scenario Overview*

| Scenario | | Central source | Backup Unit | Thermal Storage | Scenario label |
|---|---|---|---|---|---|
| Scenario X | LTDH | Waste Heat | HP | no | LTDH_X_HP |
| | | Waste Heat | HP | BTES | LTDH_X_HP_BTES |
| | | Waste Heat | HP | PTES | LTDH_X_HP_PTES |
| | ULTDH | Waste Heat | HP | no | ULTDH_X_HP |
| | | Waste Heat | HP | BTES | ULTDH_X_HP_BTES |
| | | Waste Heat | HP | PTES | ULTDH_X_HP_PTES |
| | NTDH | Waste Heat | HP | no | NTDH_X_HP |
| | | Waste Heat | HP | BTES | NTDH_X_HP_BTES |
| | | Waste Heat | HP | PTES | NTDH_X_HP_PTES |
| | Natural Gas | Boiler | - | - | Gas_apartments |
| | | Boiler | - | - | Gas_household |
| | | Boiler | - | - | Gas_DH |
| Scenario Y | LTDH | Waste Heat | HP | no | LTDH_Y_HP |
| | | Waste Heat | HP | BTES | LTDH_Y_HP_BTES |
| | | Waste Heat | HP | PTES | LTDH_Y_HP_PTES |
| | ULTDH | Waste Heat | HP | no | ULTDH_Y_HP |
| | | Waste Heat | HP | BTES | ULTDH_Y_HP_BTES |
| | | Waste Heat | HP | PTES | ULTDH_Y_HP_PTES |
| | NTDH | Waste Heat | HP | no | NTDH_Y_HP |
| | | Waste Heat | HP | BTES | NTDH_Y_HP_BTES |
| | | Waste Heat | HP | PTES | NTDH_Y_HP_PTES |
| | Natural Gas | Boiler | - | - | Gas_apartments |
| | | Boiler | - | - | Gas_household |
| | | Boiler | - | - | Gas_DH |
| Scenario Z | LTDH | Waste Heat | HP | no | LTDH_Z_HP |
| | | Waste Heat | HP | BTES | LTDH_Z_HP_BTES |
| | | Waste Heat | HP | PTES | LTDH_Z_HP_PTES |
| | ULTDH | Waste Heat | HP | no | ULTDH_Z_HP |
| | | Waste Heat | HP | BTES | ULTDH_Z_HP_BTES |
| | | Waste Heat | HP | PTES | ULTDH_Z_HP_PTES |
| | NTDH | Waste Heat | HP | no | NTDH_Z_HP |
| | | Waste Heat | HP | BTES | NTDH_Z_HP_BTES |
| | | Waste Heat | HP | PTES | NTDH_Z_HP_PTES |
| | Natural Gas | Boiler | - | - | Gas_apartments |
| | | Boiler | - | - | Gas_household |
| | | Boiler | - | - | Gas_DH |

### 2.5.1. Input data

The method was tested using a case study of an urban waste heat source and DH system in the City of Zagreb, Croatia. The study utilized outdoor temperature data representative of a typical meteorological year for Zagreb. This data was provided at an hourly level and obtained from NASA POWER Data Access Viewer [23].

Figure 9 shows the hourly temperature values recorded throughout the year.

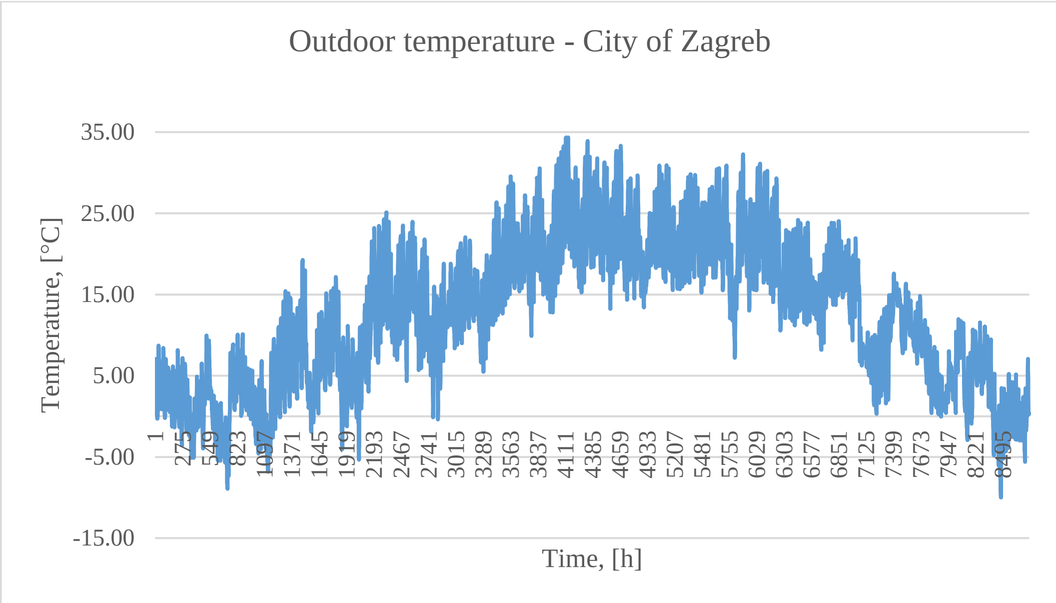


*Figure 9 Outdoor temperature distribution - City of Zagreb*

Space heating and relative domestic hot water (DHW) demand were modelled according to the total SH and DHW demand of households in Croatia in 2021 [24]. Figure 10 shows relative DH and DHW demand throughout the year.

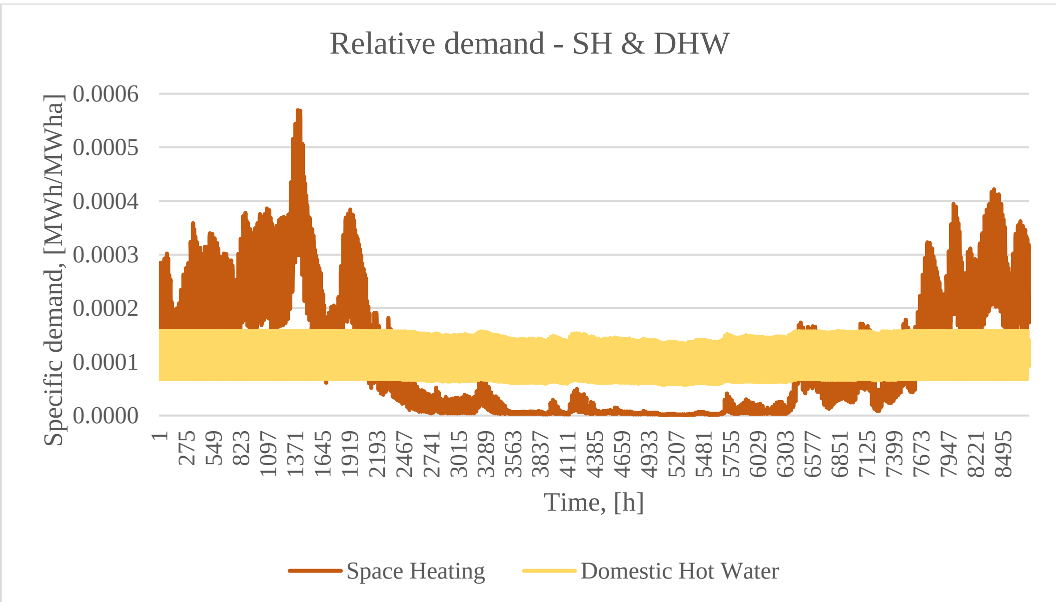


*Figure 10 Relative space heating and domestic hot water demand curve* [24]

The distribution of demand for heating and DHW was obtained through the spatial allocation of aggregated data using georeferenced databases of land coverage and/or population density. More details on the method can be found in [15].

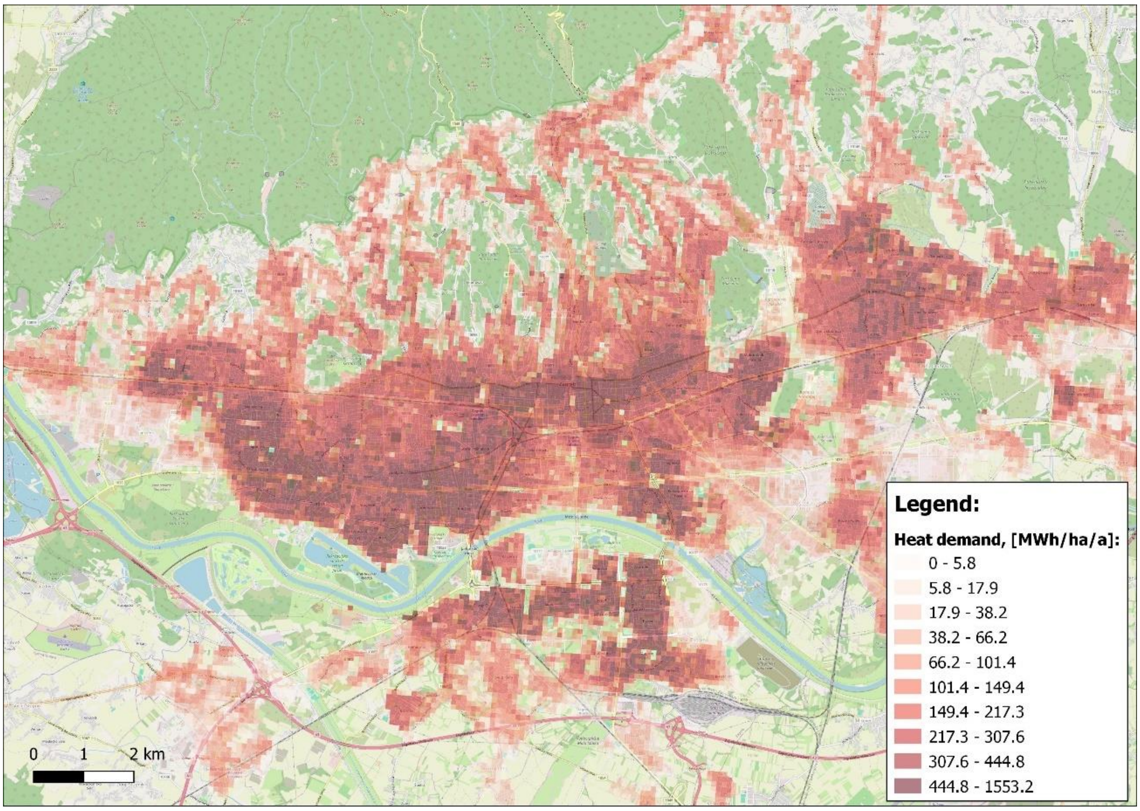


*Figure 11 Heat demand - City of Zagreb* [15]

Figure 11 shows the total HD distribution for the City of Zagreb in the field with a resolution of 250x250 m.

Three different temperature regimes have been established for the DH network: LTDH, ULTDH, and NTDH. Figure 12 illustrates these temperature regimes based on outdoor temperatures.

In the LTDH scenario, the highest supply temperature reaches 60°C. Conversely, the NTDH scenario has the lowest supply temperature at 20°C. It is noted that when the outdoor temperature falls below 10°C, the supply temperature begins to rise linearly. However, the return temperature behaves differently. At 10°C, the return temperature decreases before gradually increasing linearly as the outdoor temperature continues to drop.

The temperature curves and their corresponding equations for both supply and return lines in the ULTDH and LTDH networks have been calculated, as presented in the provided data [25]. Understanding the temperature regime patterns enables the determination of annual heat losses. This knowledge is essential for calculating the hourly coefficients of performance of HP.

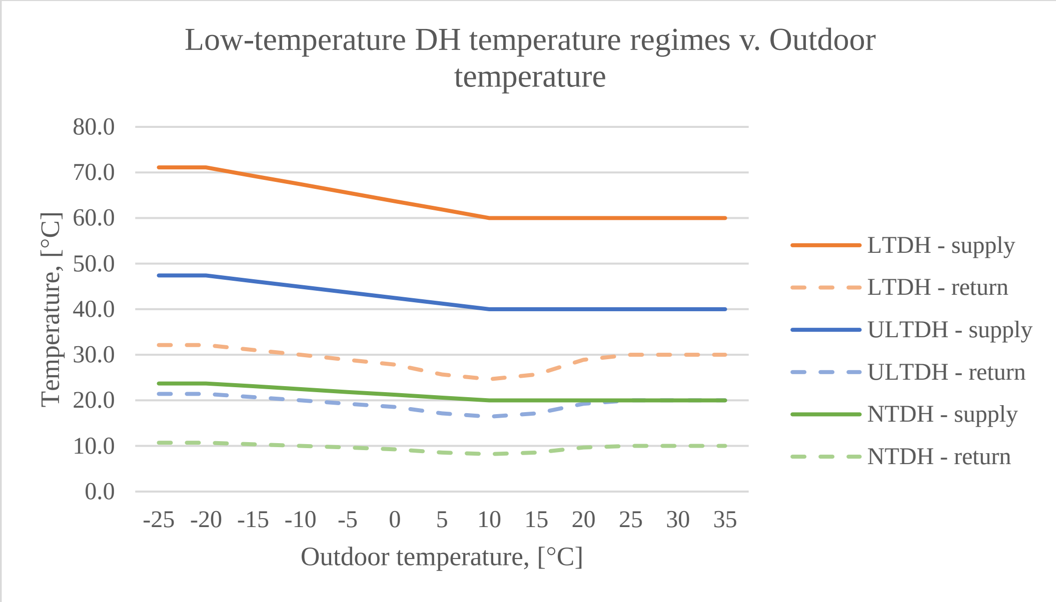


*Figure 12 Low-temperature DH temperature regimes* [25]

Figure 13 presents LTDH, ULTDH, and NTDH network temperature variations.

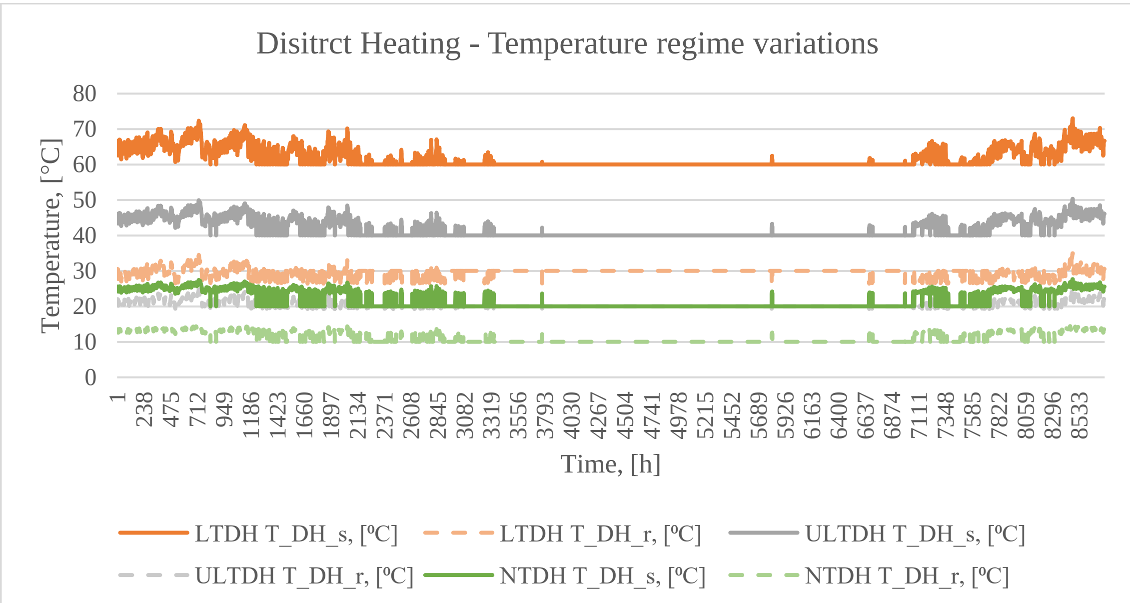


*Figure 13 Low-temperature DH temperature regimes variations* [25]

### 2.5.2. System sizing and costs

In scenarios with individual heating, total HD was divided with full load hours instead of just total DHW demand as in other cases. According to [26], [27] the full load hours are assumed as 2.000 h/annually. To calculate the number of decentral units, the fixed capacity of one unit was determined. Values for individual gas boilers for households are 14 kW, for apartments 400 kW, and for natural gas-based DH is 5 MW [28]. Investment costs in central, backup, and individual units and TES and their expected lifetime are listed in Table 2.

*Table 2 Configuration components - Investment cost*

| Technology | Investment cost, [kW/€] | Lifetime, [years] | Reference |
|---|---|---|---|
| Central WHHP | $867 \cdot Q_{central}^{-0.1418}$ | 25 | [28] |
| Backup HP | $1.112 \cdot Q_{backup}^{-0.23105}$ | 25 | [28] |
| Gas boiler – household | 0,0035 | 20 | [28], [29] |
| Gas boiler – apartments | 0,015 | 25 | [28], [29] |
| Gas boiler – DH | 0,02 | 25 | [28], [30] |

Variable and fixed annual operation and maintenance costs (O&M) for each component are given in Table 3.

*Table 3 Configuration components – O&M costs*

| Technology | Fixed O&M, [€/kW] | Variable O&M, [€/kWh] | Reference |
|---|---|---|---|
| Central WHHP | 2.030.000,00 | 1.830,00 | [28] |
| Backup HP | 2.030.000,00 | 1.830,00 | [28] |
| Gas boiler – household | 13,45 | 47,6 | [28], [29] |
| Gas boiler – apartments | 1,65 | 47,6 | [28], [29] |
| Gas boiler – DH | 0,4146 | 47,6 | [28], [30] |

The DH network was sized according to the given data [31], [32] The network costs were determined as a function of network length and pipe diameters, as shown in Figure 14.

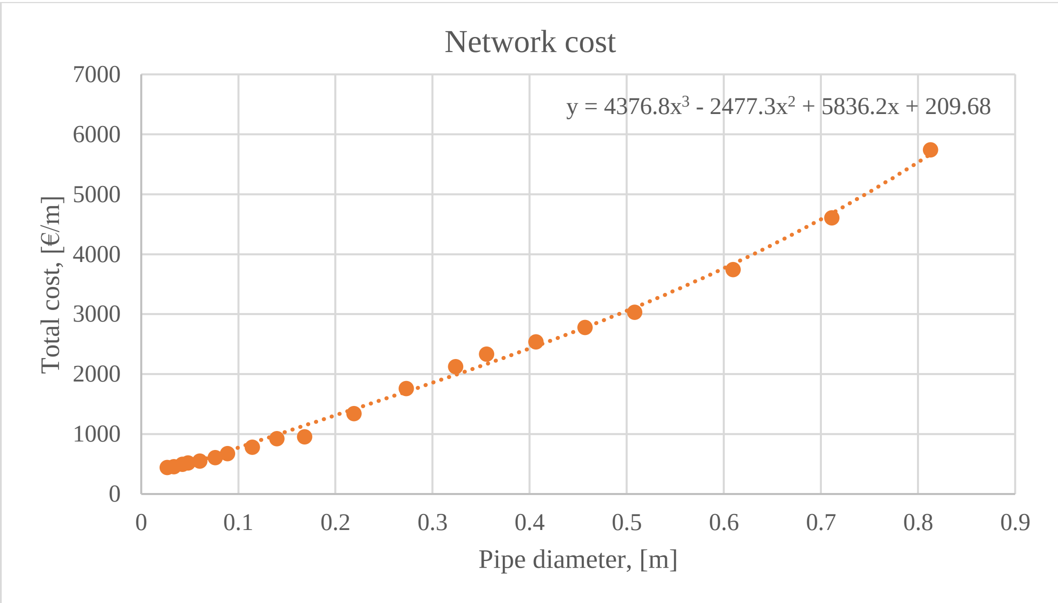


*Figure 14 Network cost as a function of the diameter and length*

Network lifetime was assumed to be 30 years [32]. The network's annual O&M costs were assumed to be 0,6% of the total investment cost in the network [31].

PTES and BTES were sized according to data given in [28]. The specific cost of TES was determined as a function of the size of the storage. Figure 15 shows the specific storage cost.

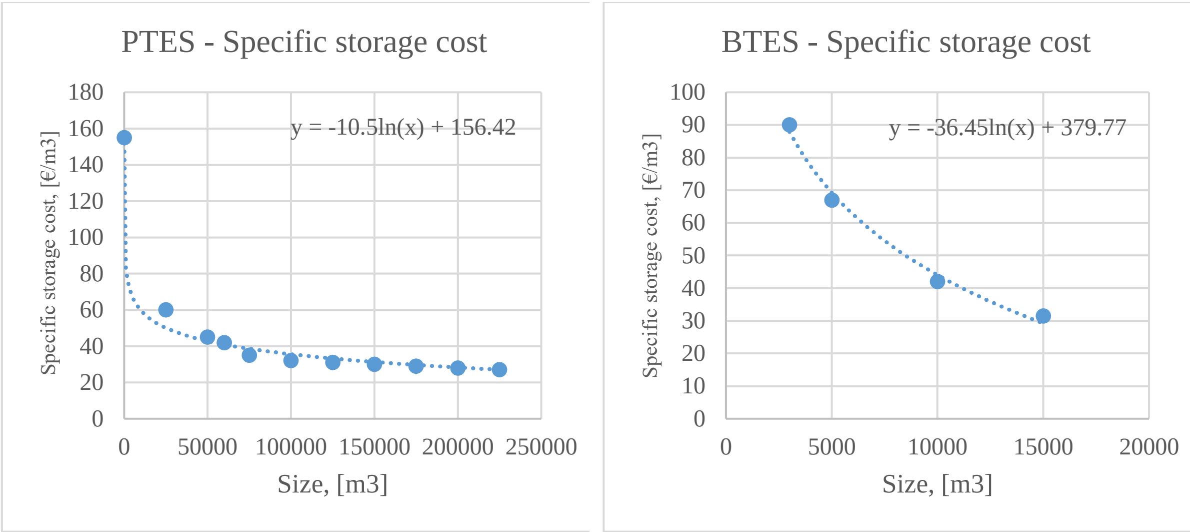


**a)** **b)**

*Figure 15 Specific storage cost: a) PTES, b) BTES* [28]

The electricity and natural gas price data utilized in this paper was sourced from [33] representing the mean electricity tariff (without taxes) applicable to both households and non-household consumers across Europe. Specifically, the recorded figures stood at 81,10 €/MWh for non-residential consumers and 126,90 €/MWh for residential consumers. Gas prices were determined based on the average rates observed in European households, amounting to 47,60 €/MWh. The cost of the Emission Trading System (ETS) was also considered, and it amounted to 57,50 €/$t_{CO2eq}$ [34].

Carbon Emission Factors, $f_{CO_2}$, and primary energy factor, $f_{prim}$, were taken from Croatian data [35]. CEF values are:

- 0,233 $tCO_2$/MWh for natural gas.
- 0,280 $tCO_2$/MWh for electricity.
- 0,212 $tCO_2$/MWh for existing DH system based on combined heat and power technology.

PEF values are:

- 1,151 for natural gas.
- 2,201 for electricity.
- 0,900 for the existing DH system based on combined heat and power technology.

## 3. Results

This Section presents the results from the four-step method, which includes spatial analysis, thermodynamic models, a DH model, and 3E analysis. The values obtained from the 3E analysis were compared to those from individual gas boiler heating systems. These systems include those for households and apartments, as well as existing natural gas-based DH systems. This comparison aims to determine the optimal configuration of the heating system.

### 3.1. Spatial analysis

Figure 16 shows the result of a spatial analysis where observed waste heat sources are located. The precise locations of these sources are marked with distinct symbols and colours. The left map provides an overview of how these sources are spatially distributed in the urban environment of the City of Zagreb, potentially supporting district heating systems that can capture and redistribute this waste heat to meet heating needs in nearby areas. The right map shows a detail from the left map at a higher map scale.

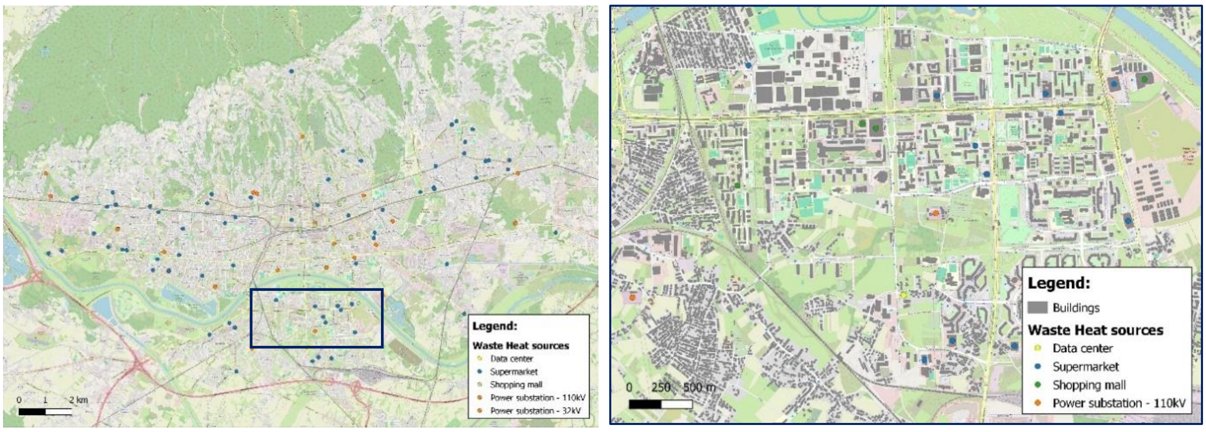


*Figure 16 City of Zagreb – Identified urban waste heat sources*

Figure 17 shows an HD map of the City of Zagreb complements Figure 16 by showing heat demand intensity across urban area, measured in MWh/ha/a. The heat demand is classified into several categories, ranging from 0 to over 1.500 MWh/ha/a, with darker red indicating higher heat demand. The highest demand is concentrated in densely populated urban areas, particularly in the inner city. Figure 17 provides data for identifying areas where urban waste heat recovery would be most beneficial. By overlaying urban waste heat sources shown in Figure 16 with HD, one can identify optimal locations for integrating waste heat into the DH network.

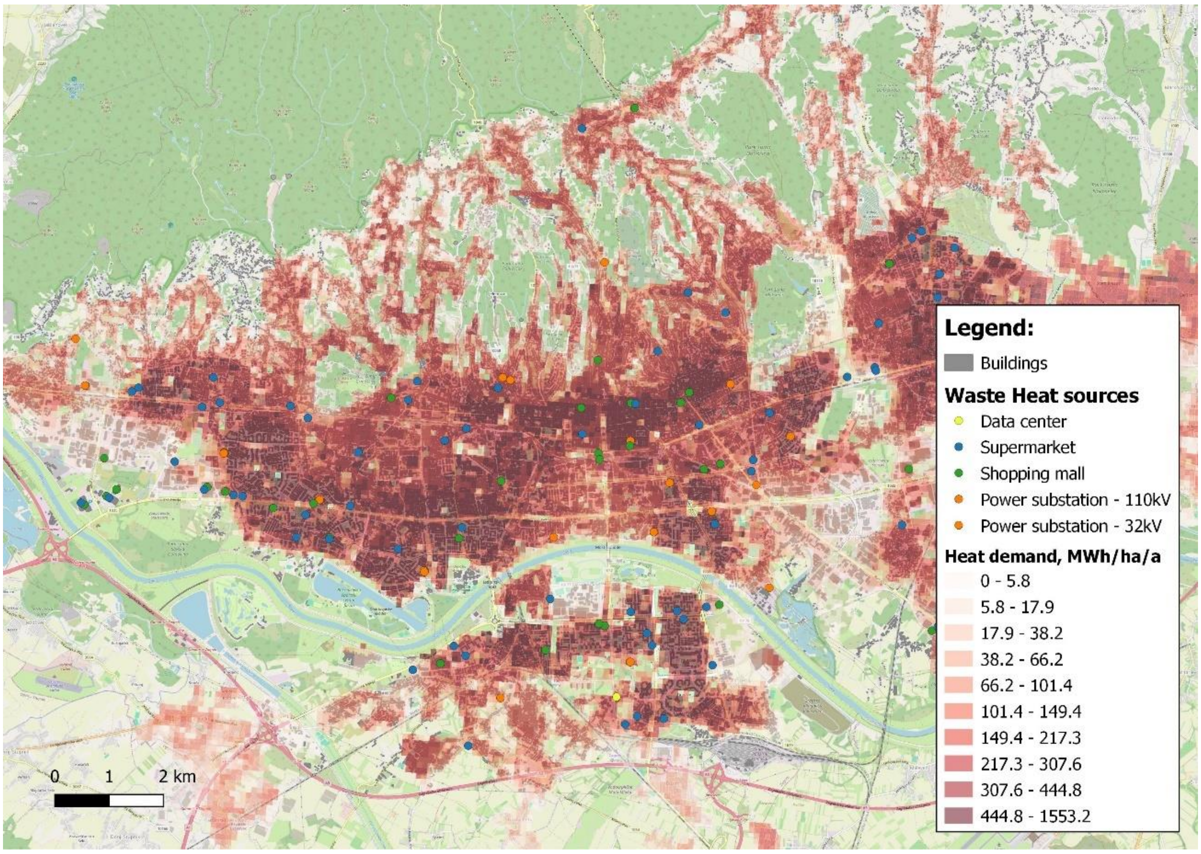


*Figure 17 Spatial distribution of waste heat sources considering heat demand*

### 3.1.1. Plot ratio

Figure 18 shows the PR results obtained through spatial analysis following the method described in Subsection 2.1. The figure presents the outcomes of all three scenarios: Scenario X, Y, and Z. PR represents the ratio of the total building area within the district to the total district area. PR values can range from 0 to 2.

Lower PR values (between 0 and 1) indicate areas where the proportion of building area is low relative to the district. This corresponds to peripheral, semi-urban areas in the case study with lower population density. On the other hand, higher PR values (from 1 to 2) indicate a higher proportion of building area, typical of highly built-up urban areas with a dense population.

The PR is represented by a gradient of blue shades in the figure. Darker shades indicate a higher PR, while lighter shades represent a lower PR.

From the results in Figure 18, it is visible that as the district area expands, the total floor area of buildings does not always increase proportionally. This results in a lower PR, suggesting less intensive land use. In areas with lower population density or less dense development, such as suburban zones, increasing the district area can lead to a decrease in PR. Conversely, in densely populated urban zones with high development intensity, expanding the district area leads to an increase in the total floor area, causing a higher PR. This indicates more intensive land use.

In rapidly growing urban areas, such as central Zagreb, there's pressure to accommodate more residents and businesses within limited space. As the district area expands, PR may increase as more buildings are constructed to meet demand.

The figure also reveals the frequency of certain results, i.e., how often specific PR values occur. Based on Figure 18, it can be observed that as the district area increases, the resolution of results decreases. This means fewer distinct PR values, as seen in Scenario Z. In contrast, reducing the district area leads to a higher resolution and more frequent repetition of specific PR values, as shown in Scenario Y.

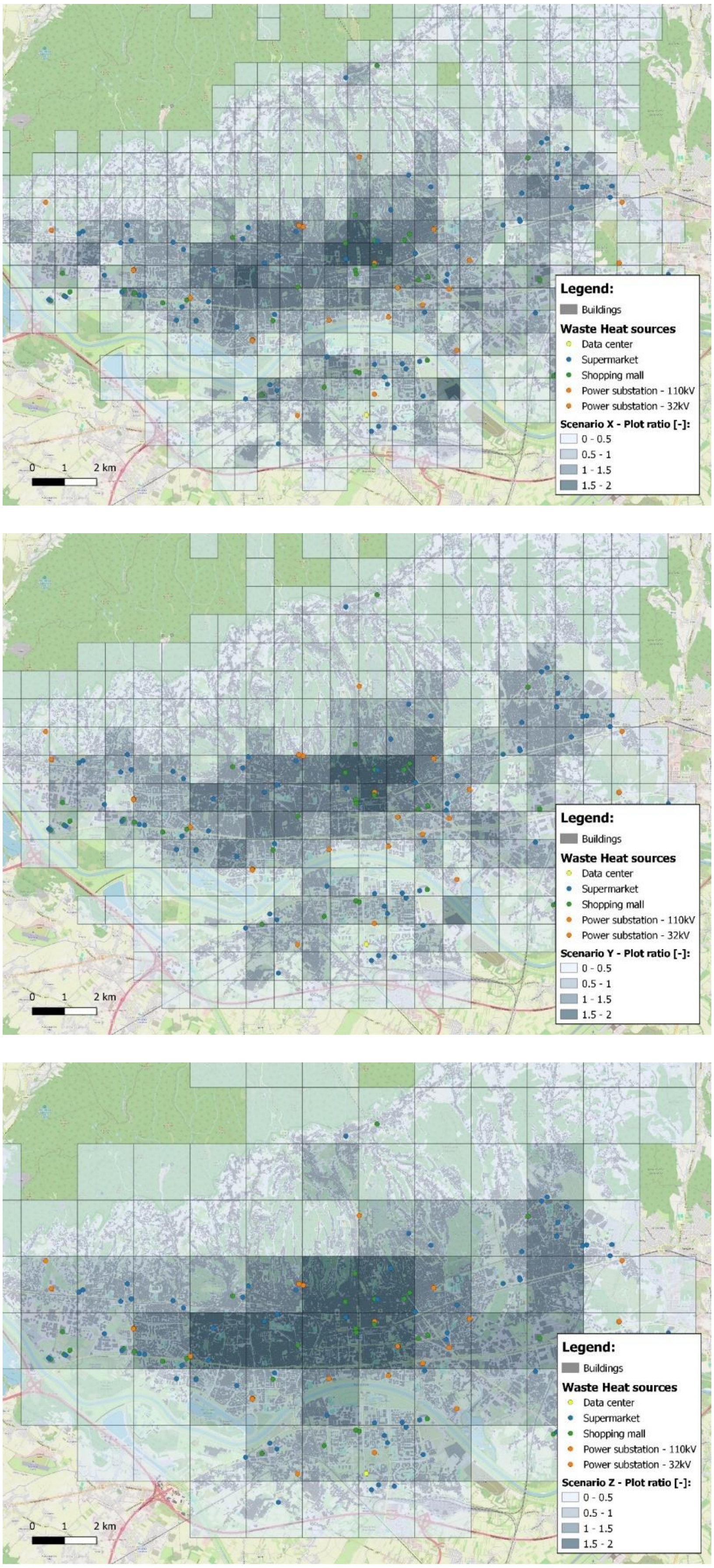


**Scenario X**

**Scenario Y**

**Scenario Z**

*Figure 18 Plot ratio – City of Zagreb*

#### 3.1.2. Heat demand

Figure 19 presents the total HD for SH and DHW preparation, considering Scenario X, Y, and Z. Figure 11, by comparison, shows the total HD when the district area is 1 hectare. These results allow us to assess variations in heat requirements across different districts.

The HD was visualized using a graduated colour scheme. Lighter shades of red indicate lower HD, while darker shades represent higher HD. Scenario X provided high-resolution results, offering detailed insights into the distribution of HD. In contrast, Scenario Z used a lower resolution, resulting in less detailed data.

The analysis revealed notable patterns in HD across the studied area. In Scenario X, where higher resolution was used, finer variations in HD were observed. This allowed for a more precise identification of areas with particularly high or low HD. Conversely, Scenario Z, with its lower resolution, gave a broader overview of HD distribution. However, it lacked the granularity seen in Scenario X. Scenario Y presented an intermediate level of detail, capturing moderate variations in HD across the districts.

From Figure 19, it is noticeable that HD is closely linked to the PR. In Scenario X, which featured smaller district areas, higher PRs typically indicated denser urban development. In these areas, the higher concentration of buildings led to increased HD. This is because densely populated urban regions generally require more energy for heating and cooling due to the higher number of buildings and human activities. In contrast, lower PRs in Scenario X corresponded to less densely developed areas with lower HD.

In Scenario Z, which considered larger district areas, the relationship between PR and HD was more nuanced. Higher PRs still indicated high urban density and correspondingly high HD. However, the larger district size introduced more variability in PRs. Some areas exhibited higher densities of buildings, while others had lower densities. As a result, HD in Scenario Z varied widely across different areas, reflecting the diverse urban structure of the larger district.

Scenario Y represented an intermediate case with moderately sized districts. In this scenario, PRs reflected a balance between urban density and open space. Areas with moderate PRs experienced moderate HD, striking a middle ground between the high density of Scenario X and the lower density of Scenario Z.

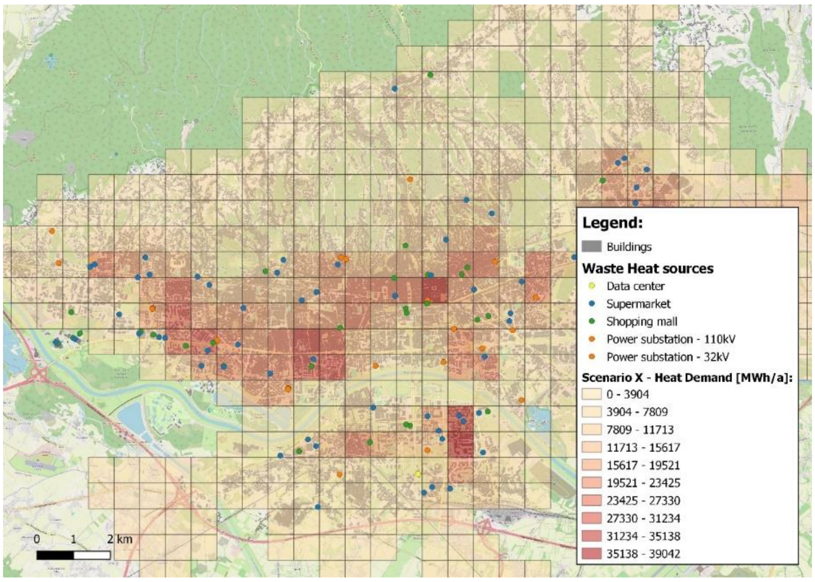


**Scenario X**

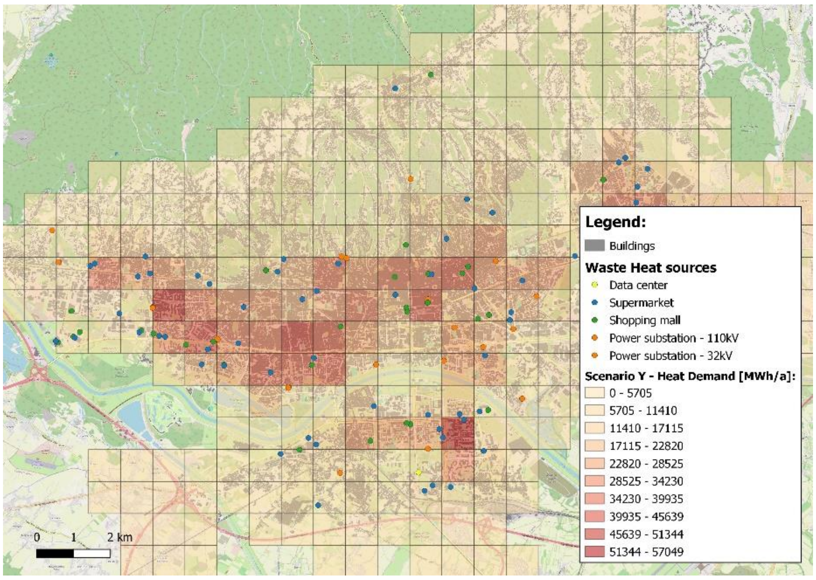


**Scenario Y**

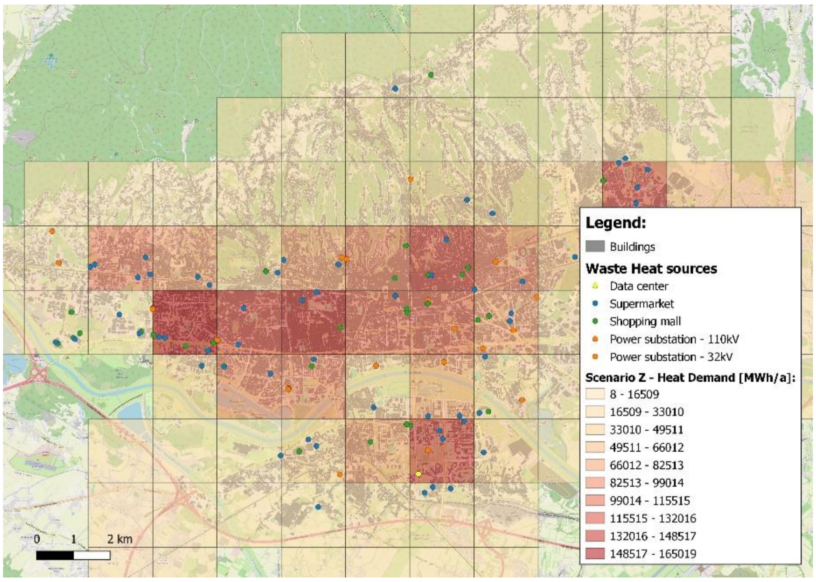


**Scenario Z**

*Figure 19 Heat demand – City of Zagreb*

#### 3.1.3. Space heating share

Figure 20 shows the $SH_S$ visually represented using a colour gradient ranging from green to red. In this scheme, green indicates areas with a low SH share, while red denotes areas with a high SH share. For example, if a district is marked in green, with an SH share of 17-28%, it means that only 17-28% of the total HD is used for space heating. The rest is allocated to DHW preparation. The SH share is a measure of building efficiency.

The SH share shown in Figure 20 reveals that the demand for space heating still outweighs the demand for DHW preparation. This can be explained by the fact that the buildings in the case study area are older and lack adequate thermal insulation. In other words, they have poorer energy performance. The situation is somewhat different in suburban areas, which are characterized by newer construction. As a result, these areas show lower SH shares, aligning with the expected results.

These findings align with the results in Figure 18 and Figure 19. In areas with higher PR**,** such as dense urban centres, higher SH values are typically observed due to increased building density and energy demand. Densely built areas tend to have more residential and commercial buildings, which leads to greater heating requirements. On the other hand, areas with lower PRs, such as suburban or rural regions, usually have lower SH shares because there are fewer buildings and lower heating demand.

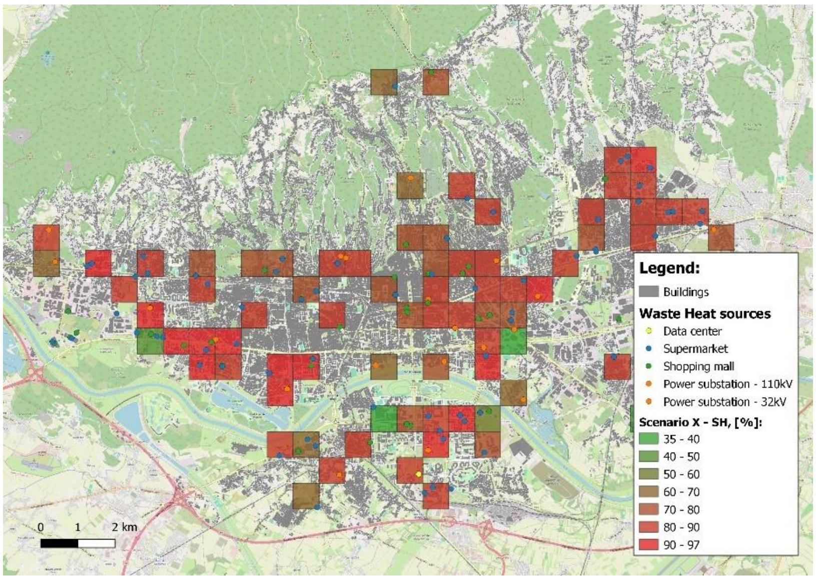


**Scenario X**

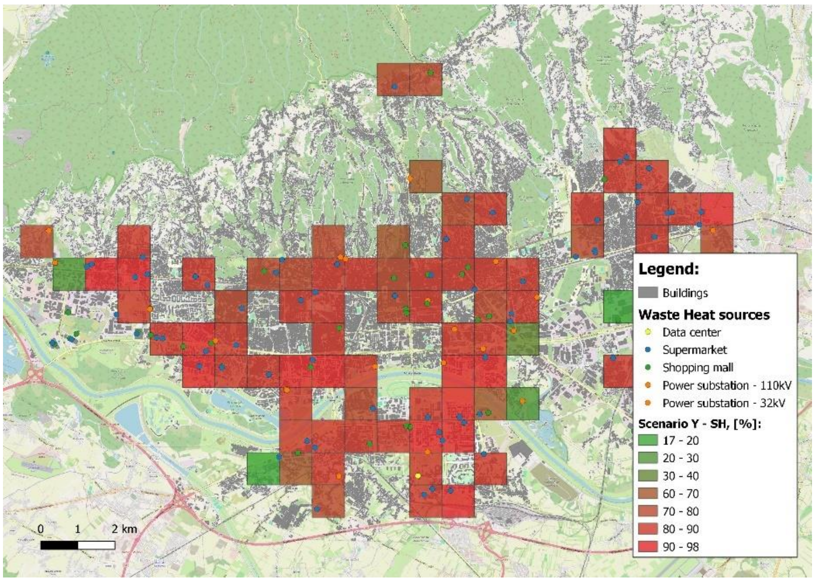


**Scenario Y**

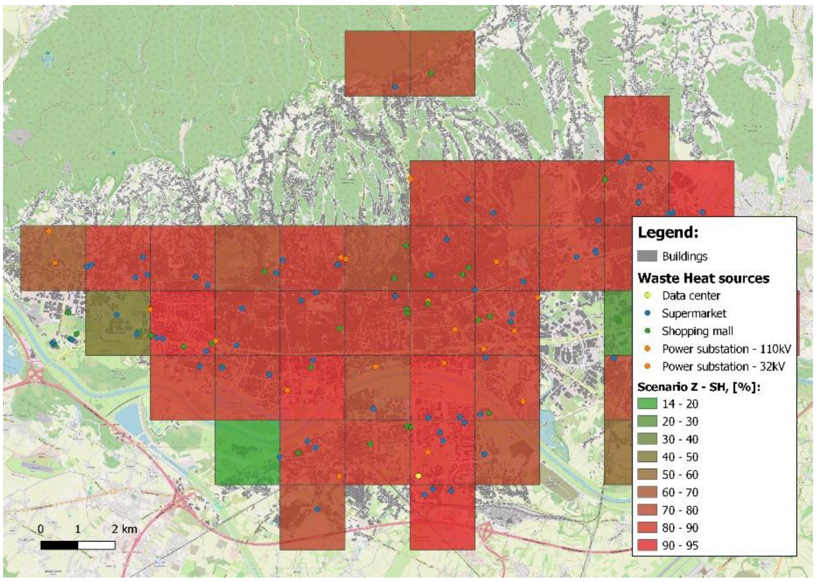


**Scenario Z**

*Figure 20 Space heating share – City of Zagreb*

### 3.2. Urban waste heat thermodynamic models

This section presents the results of the model described in Section 2. As mentioned earlier, the waste heat model for supermarket refrigeration, as well as for cooling systems of supermarkets, shopping malls, data centres, and power substations, was presented in [9], [22]. The model provides the annual hourly distribution of waste heat potential and the temperature of the waste heat source. This allows for real-time knowledge of waste heat conditions on an hourly basis throughout the year.

In Figure 21, the waste heat temperature is shown. It is observed that certain urban waste heat sources, such as cooling systems in supermarkets and shopping malls, have varying cooling loads throughout the year. This means there is no constant cooling demand year-round. From a durability perspective, cooling systems in supermarket refrigeration, data centres, and power substations are the most suitable solutions. This is because these buildings require cooling services continuously throughout the year.

The highest waste heat temperatures are achieved by supermarket refrigeration systems, with temperatures exceeding 100°C. Other waste heat sources have either low or medium temperatures, ranging between 20°C and 80°C.

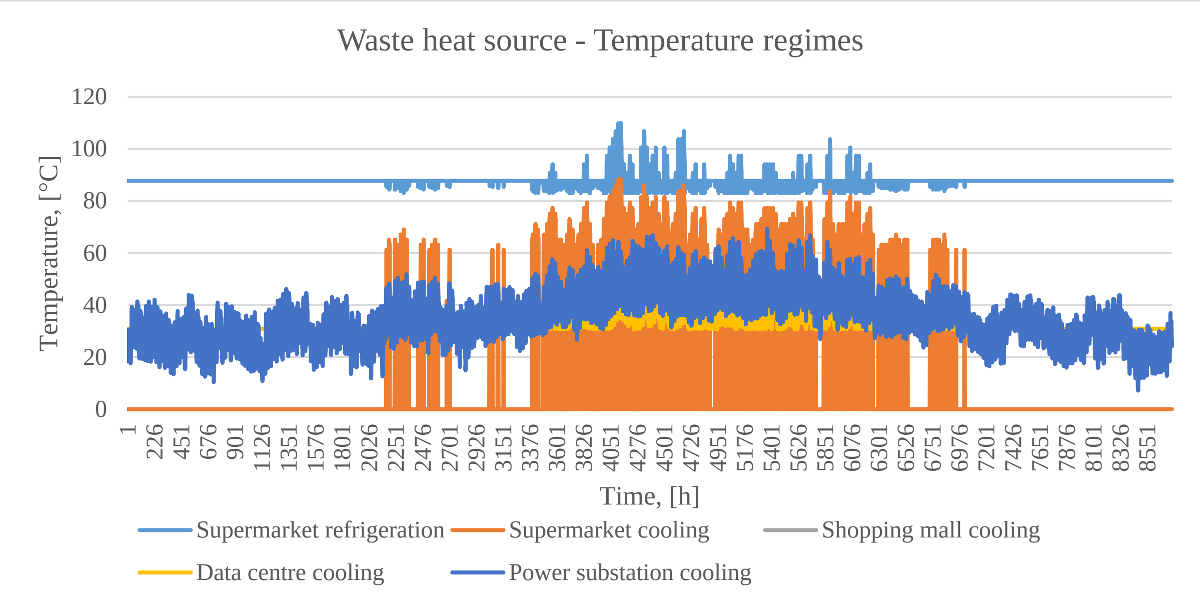


*Figure 21 Example of waste heat source temperature*

Figure 22 and Figure 23 show that the waste heat potential follows the same trend as the waste heat temperature curve. Both have a similar pattern. The cooling systems of shopping malls and supermarkets only have significant heat potential during the summer months when cooling is needed. In contrast, power substations, data centre cooling systems, and supermarket refrigeration systems generate heat potential year-round.

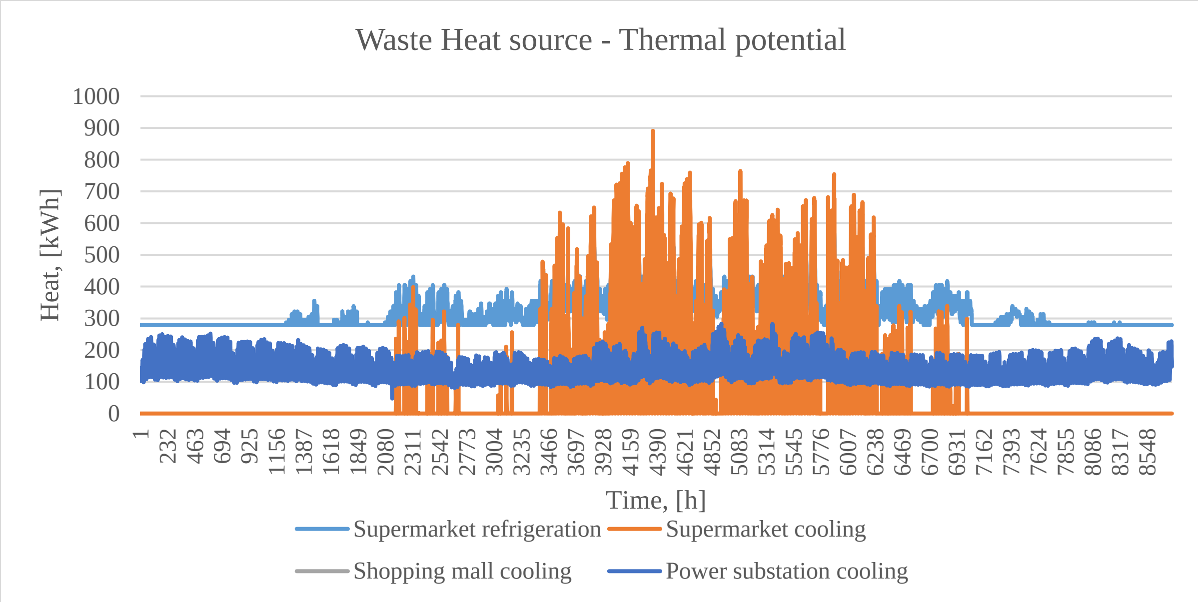


*Figure 22 Example of waste heat sources potential – supermarket refrigeration, supermarket, shopping mall & data centre cooling*

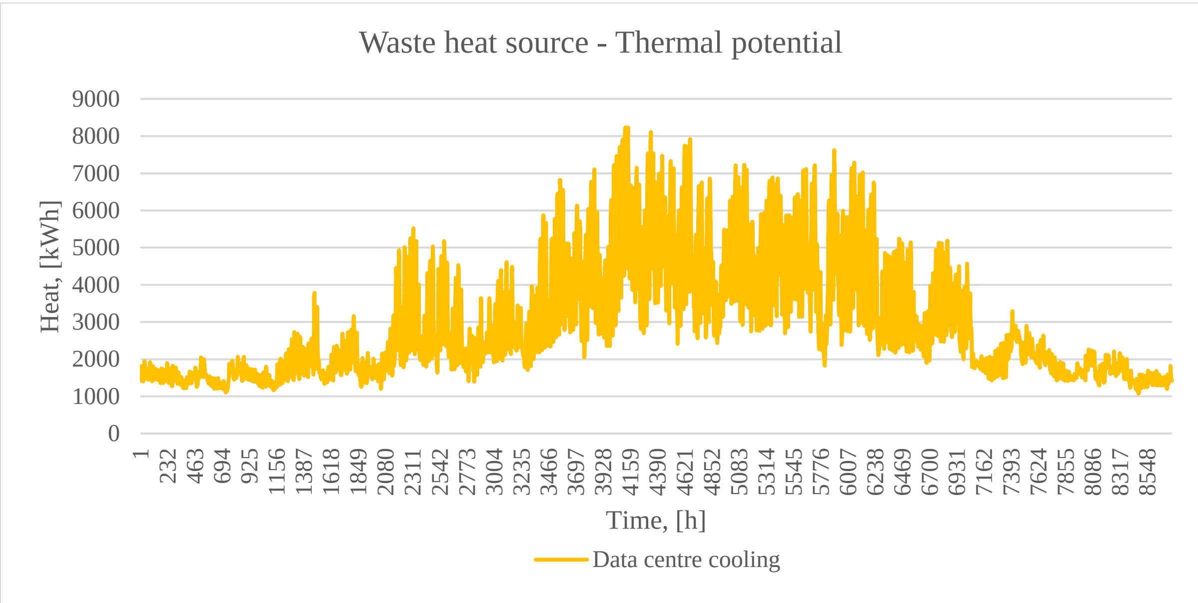


*Figure 23 Example of waste heat sources potential – data centre & power substation cooling*

Figure 24 shows urban waste heat sources, including power substations and data centres, and their waste heat potential $WH_{c\_pot}$, which could be integrated into a DH system. The thermodynamic models were incorporated into a map to visualize the possible contributions to the DH network. Each heat source was analysed individually to assess its thermal potential and temperature profile.

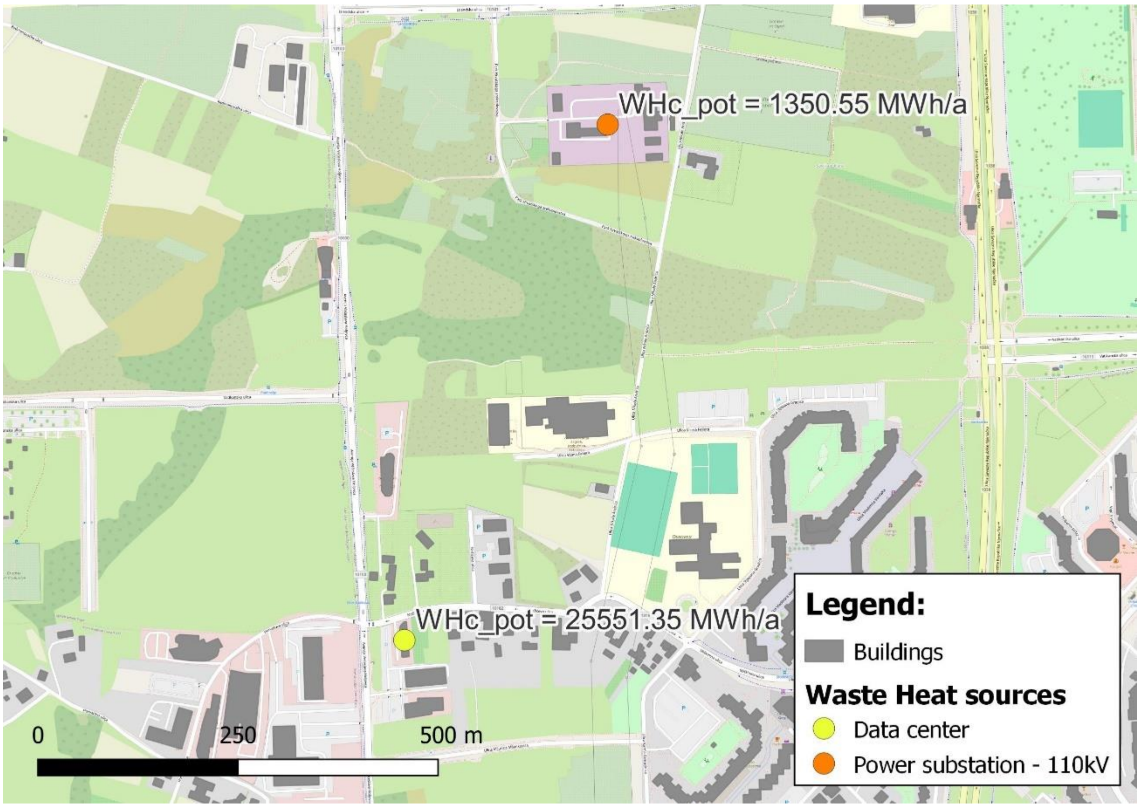


*Figure 24 Example of integrated thermodynamic model in spatial analysis*

### 3.3. DH system model & 3E Analysis

In this section, the results of the DH model and the outcomes of the 3E analysis are presented. The results of the 3E analysis are shown only for districts that contain an urban waste heat source. The presentation follows a clear sequence. First, an economic analysis was conducted for each district. Afterward, the most economically feasible solution for each district was determined and mapped.

For this economically feasible solution, the energy and environmental analysis results were then presented. When referring to the most cost-effective or least cost-effective configuration, this means the configuration with the best or worst result across all districts, i.e., the lowest or highest LCOH value. The same approach is applied to the energy and environmental analyses.

When the results mention the least or most energy-intensive configuration, this refers to the configuration with the best or worst performance across all districts, i.e., the lowest or highest PEF value. Similarly, when referring to the most carbon-intensive or least carbon-intensive configuration, this denotes the configuration with the highest or lowest CEF value across all districts.

#### 3.3.1. Economic analysis

Figure 25 compares the economic outcomes for three scenarios (X, Y, and Z) using the LCOH method. Figure 26 highlights the most cost-effective solutions for each district based on the scenarios.

In Scenario X, the economic analysis indicates that the LCOH ranges from 48,86 €/MWh (most cost-effective solution) to 65,50 €/MWh (least cost-effective solution). The most cost-effective cases correspond to configuration X_NTDH_HP, while the least cost-effective is Gas_ apartments.

In Scenario Y, the economic analysis shows that the LCOH varies from 48,13 €/MWh (most cost-effective solution) to 65,57 €/MWh (least cost-effective solution). The most cost-effective cases correspond to configuration Y_LTDH_HP, while the least cost-effective is Gas_ apartments.

In Scenario Z, the economic analysis reveals that the LCOH ranges from 43,3 €/MWh (most cost-effective solution) to 64,5 €/MWh (least cost-effective solution). The most cost-effective cases correspond to configuration Z_NTDH_HP_BTES, while the least cost-effective cases are Gas_ apartments.

Comparing the solutions it is visible that Scenario Z generally provides the lowest LCOH values across all configurations, indicating a more economically favourable outcome compared to Scenarios X and Y. Furthermore, configurations involving NTDH combined with HPs and BTES tend to yield the most cost-effective results in terms of economic viability. Conversely, configurations relying solely on gas-based solutions, such as Gas_ apartments or Gas_DH, are associated with higher LCOH values, indicating higher costs and less economic efficiency. Therefore, Scenario Z, particularly configurations involving NTDH with HP and BTES, emerges as the most favourable option for achieving lower LCOH and low-temperature DH expansion and, consequently, greater economic feasibility regarding the set boundary conditions.

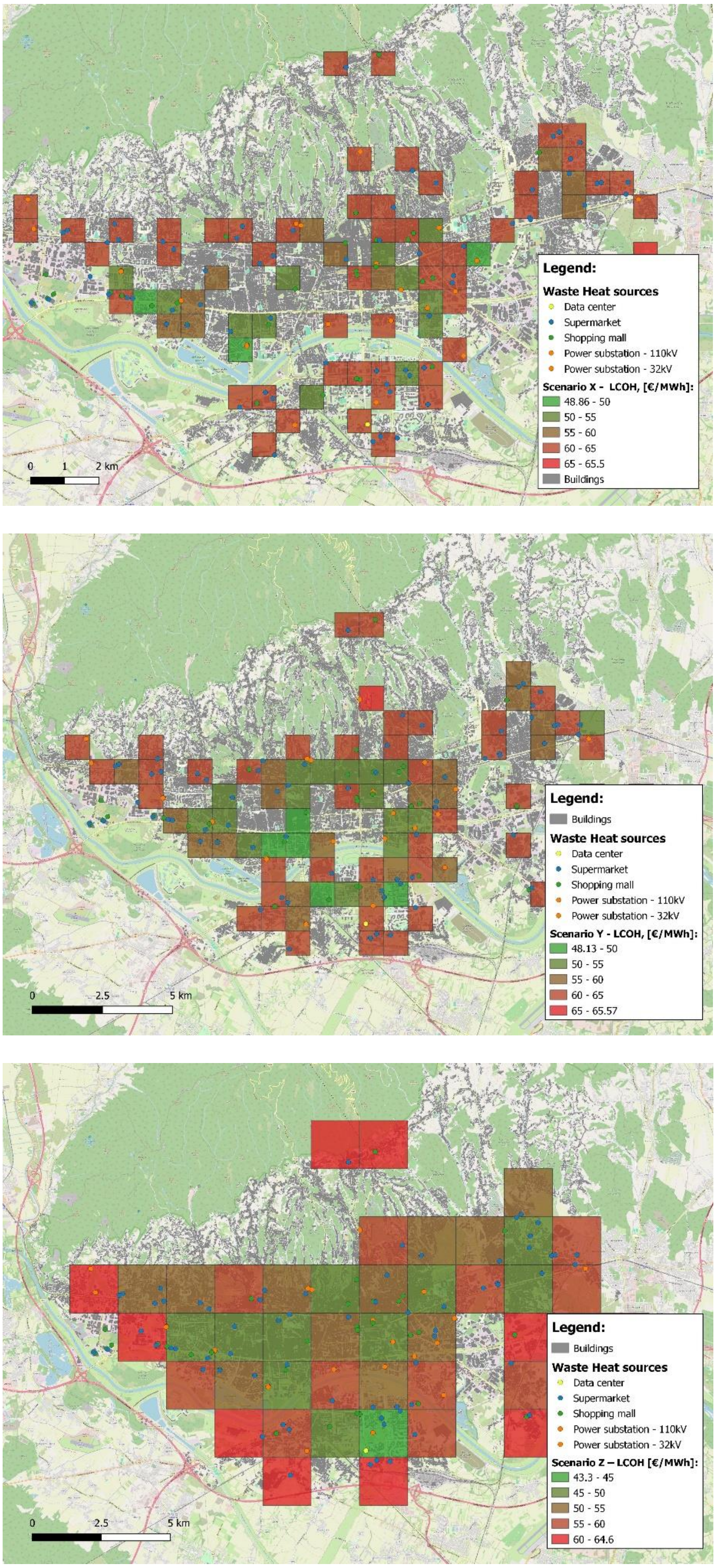


**Scenario X**

**Scenario Y**

**Scenario Z**

*Figure 25 Levelized Cost of Heat – City of Zagreb*

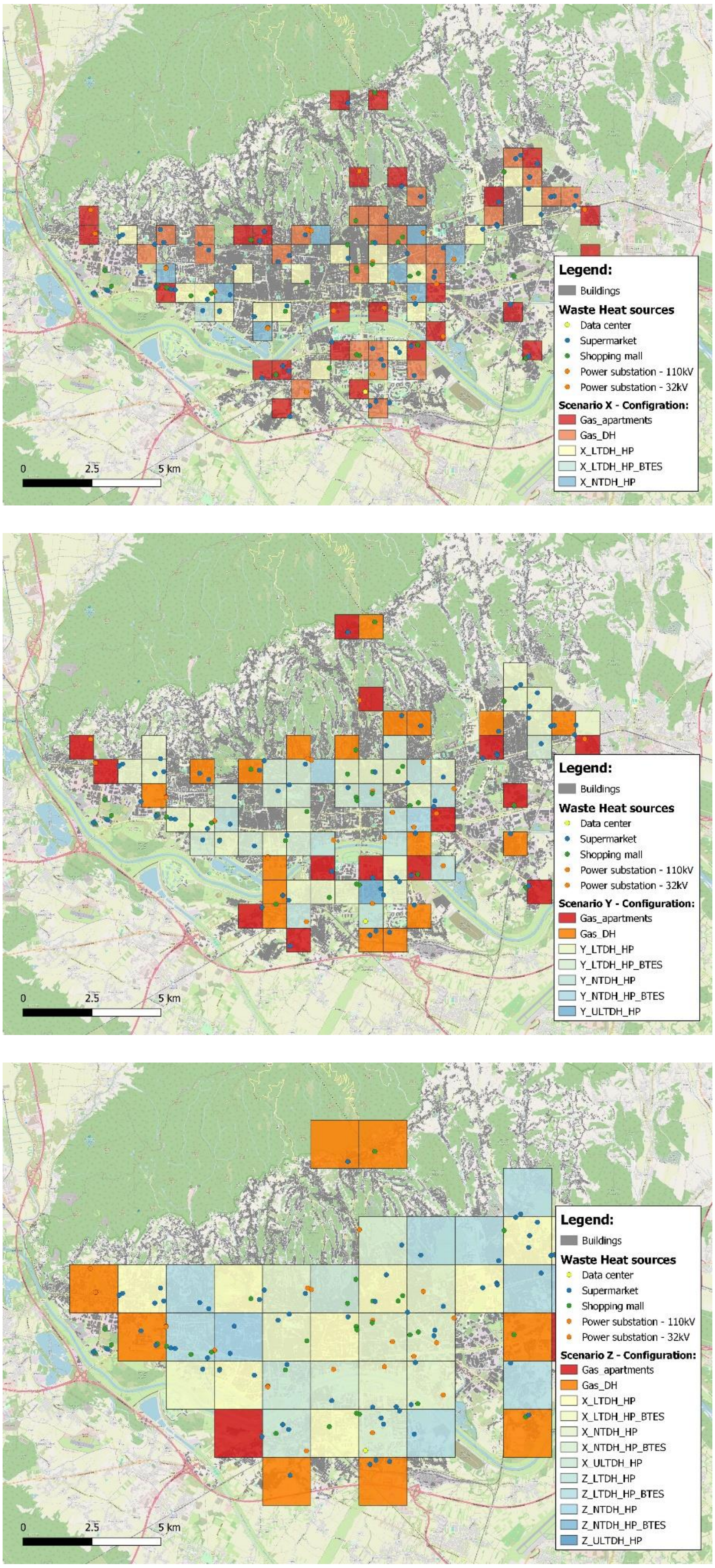


**Scenario X**

**Scenario Y**

**Scenario Z**

*Figure 26 Optimal configuration – City of Zagreb*

### 3.3.2. Energy analysis

The analysis of Figure 27 comparing Scenarios X, Y, and Z provides insights into the efficiency of different DH configurations, measured by the PEF. The PEF is an indicator of how much primary energy is required to cover HD. Lower PEF values represent more energy-efficient solutions, meaning less primary energy is used to meet the heating requirements.

In Scenario X, the PEF values range from 0,910 to 1,140, indicating the spectrum of energy efficiency across the various heating solutions. The lowest PEF value (0,910) corresponds to the configuration X_NTDH_HP (low-temperature district heating with heat pumps), which is the least energy-intensive and most efficient solution. On the opposite end, the gas-based heating solution for apartments has a PEF of 1,140, representing the highest energy intensity and the least optimal solution in this scenario.

In Scenario Y, the PEF values range from 0,841 to 1,140, showing a broader range of energy efficiencies compared to Scenario X. The configuration Y_NTDH_HP, which similarly utilizes low-temperature DH with heat pumps, achieves the best energy efficiency with the lowest PEF of 0,841. Again, gas-based heating solutions are at the upper limit of energy intensity, with a PEF of 1,140. This scenario demonstrates a greater potential for energy savings, as the lower PEF values indicate that less primary energy is consumed for heat demand compared to Scenario X.

Scenario Z presents the most favourable results, with PEF values ranging from 0,827 to 1,140. The least energy-intensive configuration in this scenario is Z_NTDH_HP_BTES, which combines low-temperature DH, heat pumps, and BTES. This configuration achieves the lowest PEF of 0,827, reflecting the highest energy efficiency across all scenarios. Gas-based heating again represents the least optimal solution with a PEF of 1,140, but Scenario Z demonstrates the greatest energy-saving potential among the three scenarios.

The comparative analysis reveals that Scenario Z consistently performs better than Scenarios X and Y in terms of primary energy efficiency. The integration of BTES with low-temperature DH and heat pumps in Scenario Z significantly reduces energy consumption, making it the most optimal solution. On the other hand, gas-based heating solutions show the highest energy intensity across all scenarios, indicating their lower efficiency. Scenario Z’s consistently lower PEF values highlight its superior performance and greater potential for primary energy savings, positioning it as the most energy-efficient solution overall.

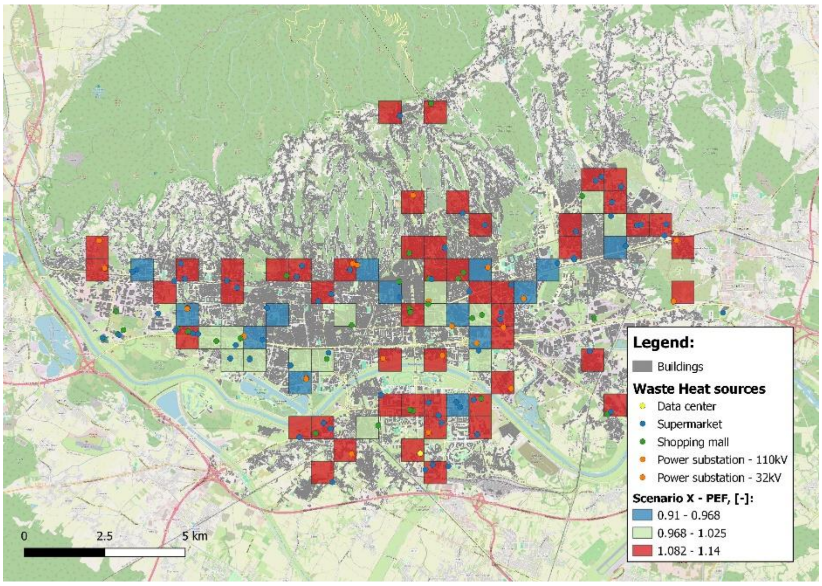


**Scenario X**

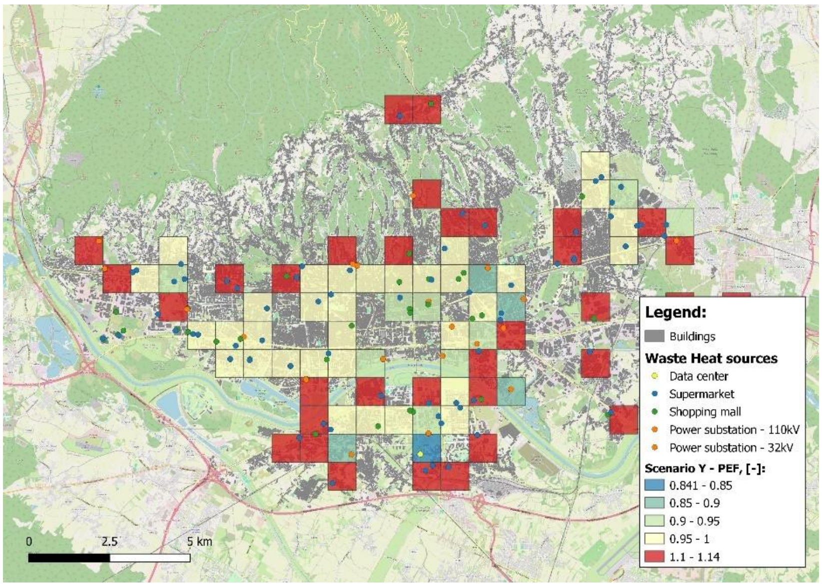


**Scenario Y**

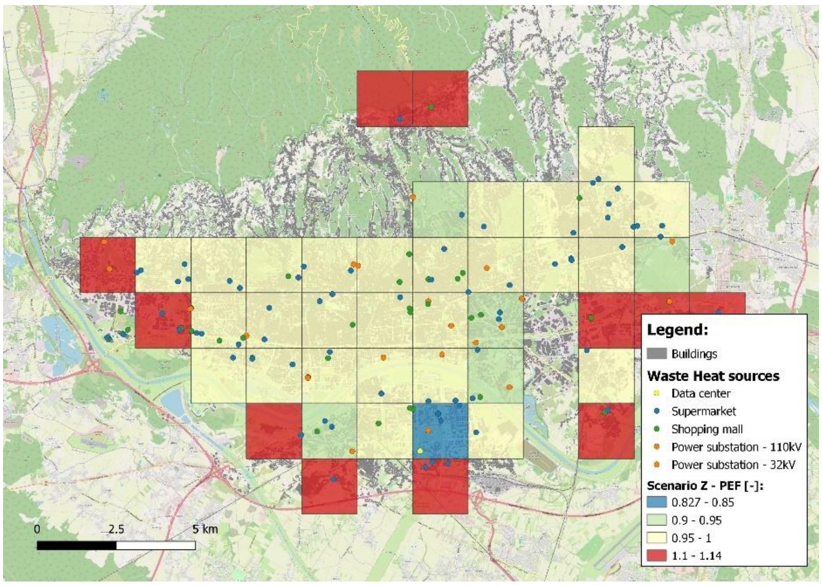


**Scenario Z**

*Figure 27 Primary Energy Factor – City of Zagreb*

### 3.3.3. Environmental analysis

The analysis of the CEF across Scenarios X, Y, and Z reveals insights into the carbon performance of different DH configurations, highlighting the environmental impact of various energy systems and technologies. Figure 28 provides a comparison of these scenarios using the CEF analysis.

In Scenario X, the CEF values span from 0,120 to 0,240 t$CO_2$ /MWh, showing a clear variation in carbon intensity. The least carbon-intensive configurations, such as X_LTDH_HP and X_NTDH_HP, indicate that lower-temperature district heating combined with HP has a significant potential to reduce $CO_2$ emissions. In contrast, gas-based apartment configurations emerge as the most carbon-intensive, contributing substantially to emissions. This suggests that shifting from gas-based systems to renewable or heat pump-based configurations can reduce carbon intensity in urban heating.

Similarly, Scenario Y presents a range of CEF values, from 0,107 to 0,241 t$CO_2$ /MWh. The configurations with Y_NTDH_HP are among the most favourable in terms of emissions, reflecting that medium-temperature district heating combined with heat pumps also offers low-carbon solutions. Again, gas-based systems continue to exhibit the highest carbon intensity, reinforcing the environmental inefficiency of traditional gas-heating systems.

Scenario Z, which incorporates more advanced technologies like BTES, provides a wider but more favourable range of CEF values, from 0,106 to 0,241 t$CO_2$/MWh. The integration of Z_NTDH_HP_BTES highlights the potential of combining medium-temperature district heating with storage technologies to achieve the lowest carbon emissions. This scenario consistently shows better performance, demonstrating that configurations incorporating BTES outperform others in reducing $CO_2$ emissions.

Comparing the three scenarios, Scenario Z emerges as the most environmentally favourable, as it provides the lowest carbon intensity configurations. This indicates that the deployment of innovative technologies such as BTES, alongside NTDH and HP, results in a marked reduction in carbon emissions, particularly when compared to conventional gas-based systems.

The analysis emphasizes the significant environmental benefits of transitioning to low- and medium-temperature district heating systems combined with heat pumps and energy storage solutions. As seen across the scenarios, configurations that rely on gas-based heating are consistently the most carbon-intensive, indicating the need for a shift toward more sustainable alternatives. Scenario Z stands out for its integration of advanced technologies that promote greater efficiency and lower carbon emissions, offering a pathway toward a more sustainable and climate-friendly DH system.

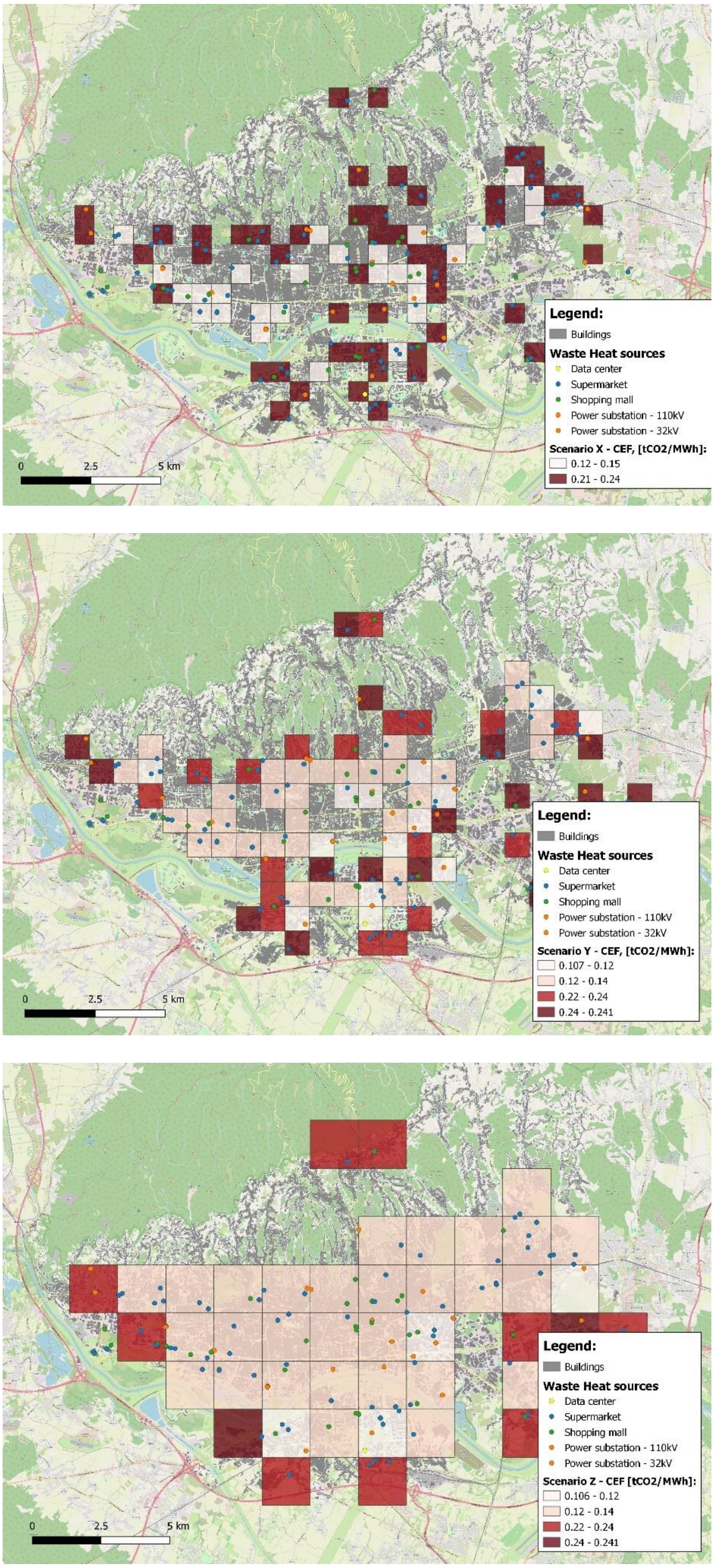


**Scenario X**

**Scenario Y**

**Scenario Z**

*Figure 28 Carbon Emission Factor - City of Zagreb*

## 4. Discussion

This paper presents a novel holistic method to assess the economic costs, as well as the energy and environmental benefits, of integrating urban waste heat sources into low-temperature DH systems. The method considers various boundary conditions. It also compares the results to gas-based heating systems, including individual gas boilers for households and apartments, as well as DH systems that rely on gas boilers.

The results provide insights into the comparative economic, energy, and environmental advantages of integrating low-temperature DH systems with renewable energy and urban waste heat sources.

The economic analysis in this paper, represented by LCOH method, shows that Scenario Z, which includes NTDH systems combined with HP and BTES, emerges as the most cost-effective configuration. This finding aligns with the results presented by Meesenburg et al. in [3], and by Gudmundsson in [36], that reports values of 45-70 €/MWh for LTDH and ULTDH systems confirming their economic feasibility. Both studies demonstrated that integrating low-temperature DH systems with renewable sources, such as heat pumps, leads to lower LCOH values. This is due to their higher efficiency and reduced reliance on fossil fuels.

Similarly, in Scenario Z of this paper, the LCOH reaches as low as 43,3 €/MWh, confirming these results. In the method presented in this paper, thermal storage plays a significant role in urban waste heat integration. It reduces the need for heat production from backup units and offers greater flexibility. This is especially important due to the seasonal variability of waste heat, a factor not discussed in [3] and [36].

Conversely, the least economically favourable configurations in this paper involve gas-based solutions, such as gas for apartments or district heating (Gas_DH). These have the highest LCOH values, reaching up to 65,50 €/MWh in Scenario X. Conventional gas-based heating systems are generally more expensive due to higher fuel costs and carbon pricing. This comparison highlights the growing consensus on the economic advantages of transitioning to lower-temperature DH systems. While [3] compares LTDH and ULTDH, it does not consider gas-based heating solutions from an energy or environmental perspective. This gap is addressed by the holistic method suggested in this paper, adding another layer of novelty to the paper.

The energy performance of the three scenarios is assessed using the Primary Energy Factor (PEF). Scenario Z again demonstrates high efficiency, with PEF values ranging from 0,827 to 1,140, The most energy-efficient configuration, Z_NTDH_HP_BTES, uses the least amount of primary energy to meet heating demands. This outcome aligns with the findings of [36], which compared 4$^{th}$ and 5$^{th}$ generation DH systems. The authors in [36] found that 5$^{th}$ generation DH systems significantly reduce primary energy consumption through the integration of renewable and waste heat sources. A key difference in this paper, however, is the inclusion of thermal storage. The reduction in PEF observed in Scenario Z is largely due to the increased system flexibility and lower losses achieved through thermal storage technologies.

The Carbon Emission Factor (CEF) analysis in this paper highlights that Scenario Z offers the most environmentally friendly outcomes. It achieves CEF values as low as 0,106 $tCO_2$/MWh, particularly in configurations involving NTDH, HPs, and BTES. This finding is consistent with the conclusions of [3] and [36]. Both studies found that ULTDH and LTDH systems, when integrated with renewable energy, substantially reduce $CO_2$ emissions compared to conventional gas-based systems. Transitioning from gas-based systems to low-temperature DH significantly lowers carbon intensity. This is evident in this paper, where gas-based systems show the highest CEF values, up to 0,241 $tCO_2$/MWh. The integration of thermal storage and renewable energy sources, as demonstrated in Scenario Z, offers substantial carbon savings by reducing reliance on fossil fuel-based systems.

Other studies, such as from Rezaie and Rosen [37] or Lund et al. [38] support the findings of this research. For instance, [33] explored the potential of district energy systems to improve energy efficiency and reduce carbon emissions, while [34] advocated for the development of low-temperature district heating systems to mitigate both economic and environmental impacts. These studies, along with [3] and [36], reinforce the conclusion that Scenario Z - combining NTDH, HP, and BTES technologies - represents the most feasible and sustainable solution for district heating.

Although this paper presents a holistic method for evaluating the techno-economic feasibility of integrating urban waste heat sources into low-temperature DH systems, it has limitations. The analysis focuses solely on the central part of the DH system, specifically the production units (i.e., the supply side). The paper does not consider the final user substation, which could influence the results and should be explored further. However, in this research, it is acceptable to neglect this effect. The primary goal is to gain a better understanding of the supply side and its impact on the economic feasibility, energy performance, and environmental effects on DH systems. Additionally, since the parameters used in the proposed approach are general, this method can be applied to various case studies. While it is expected that similar results and conclusions would be drawn for other cases, the precise impact will vary from one case to another. The proposed approach allows for the quantification of these impacts for each specific case study.

The comparative analysis in this paper, together with existing literature, confirms that integrating next-generation DH systems, particularly configurations involving heat pumps and TES, provides superior economic, energy, and environmental outcomes. These systems are essential for developing sustainable DH solutions.

## 5. Conclusion

This paper has developed and applied a novel holistic method for assessing the techno-economic feasibility of integrating urban waste heat sources into low-temperature DH systems. The method considers a range of boundary conditions and provides a comprehensive analysis of economic, energy, and environmental impacts through a 3E analysis. The approach offers key insights into the comparative benefits of different DH configurations, focusing on the City of Zagreb as a case study.

The paper confirms that LTDH systems are viable for areas with low plot ratios and high heat demand, while NTDH systems are suitable for high plot ratios and high heat demand. Scenario Z, which combines NTDH, HP, and BTES, emerged as the most cost-effective solution, with the LCOH reaching as low as 43,3 €/MWh. Scenario Z demonstrated high energy efficiency, with Primary Energy Factor values ranging from 0,827 to 1,140, This efficiency is attributed to the integration of BTES, which enhances system flexibility and reduces primary energy consumption, particularly during seasonal fluctuations in waste heat availability. Scenario Z also provided the most environmentally favourable results, with Carbon Emission Factor values as low as 0,106 $tCO_2$/MWh. This reduction in carbon emissions is largely driven by the combined use of renewable energy sources and thermal storage, which substantially reduces reliance on fossil fuels. In contrast, gas-based systems exhibited the highest CEF values, up to 0,241 $tCO_2$/MWh.

Gas-based heating solutions, such as individual gas boilers and gas-based DH, were found to be the least economically and environmentally favourable options. The paper underscores the economic and environmental advantages of next-generation DH systems, which are more sustainable and cost-effective compared to conventional gas-based alternatives.

This paper presents a holistic and adaptable method for evaluating a wide range of boundary conditions and urban waste heat sources in DH systems. The method enables the quantification of impacts across different urban settings and configurations. TES is integrated into the analysis to enhance the flexibility and efficiency of DH systems. As a result, this paper provides a more comprehensive analysis of energy and environmental performance. Previous studies have not sufficiently addressed these aspects.

Although the paper mainly focuses on the supply side of DH systems, future research should also examine final user substations. This will help refine the results and account for their potential impact on the overall system. Additionally, it is important to conduct a sensitivity analysis of the DH system configuration in response to changes in prices. These include investment costs, energy prices, and waste heat costs. The proposed method is adaptable and can be applied to other case studies. Future research should validate the method in different urban environments. Furthermore, the cooling service should not be overlooked, as low-temperature DH regimes create opportunities for its implementation.

The method emphasizes the importance of strategic spatial planning, advanced thermodynamic modelling, and comprehensive economic and environmental analyses in promoting the integration of waste heat into district heating networks. By leveraging urban waste heat sources effectively, cities like Zagreb can enhance their energy efficiency, reduce carbon footprints, and move towards a more sustainable energy future.

## 6. Acknowledgments

This research has been supported by the Croatian Science Foundation's Young Researchers' Career Development Programme (DOK-02-2021). The authors gratefully acknowledge this support.

## 7. Contribution statement

**Josip Miškić**: Conceptualization, Methodology, Software, Investigation, Writing – original draft, Writing – review & editing, Visualization. **Hrvoje Dorotić**: Writing – review & editing, Supervision. **Tomislav Pukšec**: Writing – review & editing, Supervision. **Daniel Rolph Schneider**: Writing – review & editing, Supervision. **Neven Duić**: Writing – review & editing, Supervision.

## 8. References

[1] H. Lund *et al.*, "Perspectives on fourth and fifth generation district heating," *Energy*, vol. 227, p. 120520, Jul. 2021, doi: 10.1016/J.ENERGY.2021.120520.

[2] A. Volkova, I. Pakere, L. Murauskaite, P. Huang, K. Lepiksaar, and X. Zhang, “5th generation district heating and cooling (5GDHC) implementation potential in urban areas with existing district heating systems,” *Energy Reports*, vol. 8, pp. 10037–10047, Nov. 2022, doi: 10.1016/J.EGYR.2022.07.162.

[3] W. Meesenburg, T. Ommen, J. E. Thorsen, and B. Elmegaard, “Economic feasibility of ultra-low temperature district heating systems in newly built areas supplied by renewable energy,” *Energy*, vol. 191, p. 116496, Jan. 2020, doi: 10.1016/J.ENERGY.2019.116496.

[4] O. Gudmundsson, A. Dyrelund, and J. E. Thorsen, “Comparison of 4th and 5th generation district heating systems,” *E3S Web of Conferences*, vol. 246, p. 09004, Mar. 2021, doi: 10.1051/E3SCONF/202124609004.

[5] S. Buffa, M. Cozzini, M. D’Antoni, M. Baratieri, and R. Fedrizzi, “5th generation district heating and cooling systems: A review of existing cases in Europe,” *Renewable and Sustainable Energy Reviews*, vol. 104, pp. 504–522, Apr. 2019, doi: 10.1016/J.RSER.2018.12.059.

[6] A. Buonomano, C. Forzano, L. Mongibello, A. Palombo, and G. Russo, “Optimising low-temperature district heating networks: A simulation-based approach with experimental verification,” *Energy*, vol. 304, p. 131954, Sep. 2024, doi: 10.1016/J.ENERGY.2024.131954.

[7] A. M. Jodeiri, M. J. Goldsworthy, S. Buffa, and M. Cozzini, “Role of sustainable heat sources in transition towards fourth generation district heating – A review,” *Renewable and Sustainable Energy Reviews*, vol. 158, p. 112156, Apr. 2022, doi: 10.1016/J.RSER.2022.112156.

[8] M. Yuan *et al.*, “Renewable energy and waste heat recovery in district heating systems in China: A systematic review,” *Energy*, vol. 294, p. 130788, May 2024, doi: 10.1016/J.ENERGY.2024.130788.

[9] H. Dorotić, K. Čuljak, J. Miškić, T. Pukšec, and N. Duić, “Technical and Economic Assessment of Supermarket and Power Substation Waste Heat Integration into Existing District Heating Systems,” *Energies 2022, Vol. 15, Page 1666*, vol. 15, no. 5, p. 1666, Feb. 2022, doi: 10.3390/EN15051666.

[10] C. Huang, Y. Zong, S. You, C. Træholt, J. E. Thorsen, and L. F. S. Larsen, “Economical heat recovery dynamic control and business model for supermarket refrigeration system coupled with district heating system,” *Sustainable Energy, Grids and Networks*, vol. 32, p. 100800, Dec. 2022, doi: 10.1016/J.SEGAN.2022.100800.

[11] F. Giunta and S. Sawalha, “Techno-economic analysis of heat recovery from supermarket’s CO2 refrigeration systems to district heating networks,” *Appl Therm Eng*, vol. 193, p. 117000, Jul. 2021, doi: 10.1016/J.APPLTHERMALENG.2021.117000.

[12] J. Stock, T. Schmidt, A. Xhonneux, and D. Müller, “Optimisation of district heating transformation for the efficient integration of a low-temperature heat source,” *Energy*, vol. 308, p. 132461, Nov. 2024, doi: 10.1016/J.ENERGY.2024.132461.

[13] I. Brocklebank, P. Styring, and S. Beck, "Heat mapping for district heating," *Energy Procedia*, vol. 151, pp. 47–51, Oct. 2018, doi: 10.1016/J.EGYPRO.2018.09.025.

[14] C. Su, J. Dalgren, and B. Palm, "High-resolution mapping of the clean heat sources for district heating in Stockholm City," *Energy Convers Manag*, vol. 235, p. 113983, May 2021, doi: 10.1016/J.ENCONMAN.2021.113983.

[15] T. Novosel, T. Pukšec, N. Duić, and J. Domac, "Heat demand mapping and district heating assessment in data-pour areas," *Renewable and Sustainable Energy Reviews*, vol. 131, p. 109987, Oct. 2020, doi: 10.1016/J.RSER.2020.109987.

[16] J. Chambers, S. Zuberi, M. Jibran, K. Narula, and M. K. Patel, "Spatiotemporal analysis of industrial excess heat supply for district heat networks in Switzerland," *Energy*, vol. 192, p. 116705, Feb. 2020, doi: 10.1016/J.ENERGY.2019.116705.

[17] U. Persson and S. Werner, "Heat distribution and the future competitiveness of district heating," *Appl Energy*, vol. 88, no. 3, pp. 568–576, Mar. 2011, doi: 10.1016/J.APENERGY.2010.09.020.

[18] S. Nielsen and B. Möller, "GIS based analysis of future district heating potential in Denmark," *Energy*, vol. 57, pp. 458–468, Aug. 2013, doi: 10.1016/J.ENERGY.2013.05.041.

[19] F. Bühler, S. Petrović, T. Ommen, F. M. Holm, H. Pieper, and B. Elmegaard, "Identification and Evaluation of Cases for Excess Heat Utilisation Using GIS," *Energies 2018, Vol. 11, Page 762*, vol. 11, no. 4, p. 762, Mar. 2018, doi: 10.3390/EN11040762.

[20] V. Olofsson, "5th Generation District Heating and Cooling - A High-Level Simulation Model of a Novel District Energy Network," Umea, 2022.

[21] U. Persson and S. Werner, "Effective Width : The Relative Demand for District Heating Pipe Lengths in City Areas," *12th International Symposium on District Heating and Cooling, Tallinn: Tallinn University of Technology*, pp. 128–131, 2010.

[22] J. Miškić, H. Dorotić, T. Pukšec, V. Soldo, and N. Duić, "Optimization of data centre waste heat integration into the low-temperature district heating networks," *Optimization and Engineering*, vol. 25, no. 1, pp. 63–91, Mar. 2024, doi: 10.1007/S11081-023-09837-5/METRICS.

[23] "POWER | Data Access Viewer." Accessed: Apr. 11, 2024. [Online]. Available: https://power.larc.nasa.gov/data-access-viewer/

[24] O. Ruhnau, L. Hirth, and A. Praktiknjo, "Time series of heat demand and heat pump efficiency for energy system modeling," *Scientific Data 2019 6:1*, vol. 6, no. 1, pp. 1–10, Oct. 2019, doi: 10.1038/s41597-019-0199-y.

[25] S. C. Stockholm, J. F. Flores, B. Lacarrière, O. Le Corre, and V. Martin, "Study of a district heating substation using the return water of the main system to service a low-temperature secondary network," *The 14th International Symposium on District Heating and Cooling* , 2014, Accessed: Mar. 11, 2024. [Online]. Available: https://urn.kb.se/resolve?urn=urn:nbn:se:kth:diva-185715

[26] R. Segers and H. Busker, "Equivalent full load hours for heating of reversible air-air heat pumps," Den Haag/Heerlen/Bonaire, 2015.

[27] J. E. Thorsen and T. Ommen, "Field experience with ULTDH substation for multifamily building," *Energy Procedia*, vol. 149, pp. 197–205, Sep. 2018, doi: 10.1016/J.EGYPRO.2018.08.184.

[28] "Technology catalogues | The Danish Energy Agency." Accessed: Mar. 11, 2024. [Online]. Available: https://ens.dk/en/our-services/technology-catalogues

[29] "Technology Data for Individual Heating Plants | The Danish Energy Agency." Accessed: Apr. 19, 2024. [Online]. Available: https://ens.dk/en/our-services/projections-and-models/technology-data/technology-data-individual-heating-plants

[30] "Technology Data-Energy Plants for Electricity and District heating generation." [Online]. Available: http://www.ens.dk/teknologikatalog

[31] J. Kim and I. Weidlich, "Identification of Individual District Heating Network Conditions using Equivalent Full Load Cycles," *Energy Procedia*, vol. 116, pp. 343–350, Jun. 2017, doi: 10.1016/J.EGYPRO.2017.05.081.

[32] "New tool to share Danish district heating knowledge | The Danish Energy Agency." Accessed: Mar. 11, 2024. [Online]. Available: https://ens.dk/en/press/new-tool-share-danish-district-heating-knowledge

[33] "Consumer Energy Prices in Europe." Accessed: Mar. 11, 2024. [Online]. Available: https://qery.no/consumer-energy-prices-in-europe/

[34] "EU Carbon Permits - Price - Chart - Historical Data - News." Accessed: Mar. 11, 2024. [Online]. Available: https://tradingeconomics.com/commodity/carbon

[35] Ministry of Physical Planning Construction and State Assets, "Primary energy and CO2 emission factor," Zagreb, 2022.

[36] O. Gudmundsson, A. Dyrelund, and J. E. Thorsen, "Comparison of 4th and 5th generation district heating systems," *E3S Web of Conferences*, vol. 246, p. 09004, Mar. 2021, doi: 10.1051/E3SCONF/202124609004.

[37] B. Rezaie and M. A. Rosen, "District heating and cooling: Review of technology and potential enhancements," *Appl Energy*, vol. 93, pp. 2–10, May 2012, doi: 10.1016/J.APENERGY.2011.04.020.

[38] H. Lund *et al.*, "4th Generation District Heating (4GDH): Integrating smart thermal grids into future sustainable energy systems," *Energy*, vol. 68, pp. 1–11, Apr. 2014, doi: 10.1016/J.ENERGY.2014.02.089.